A study of the feasibility of ^{99}Mo production inside the TU Delft Hoger Onderwijs Reactor

A Monte Carlo serpent analysis of the HOR research reactor and its medical isotope production capabilities using uranium salts.

Kenneth Elgin

Abstract

The production of Molybdenum-99 is an area of continued international internet as its daughter isotope Technetium-99m is widely used in medical diagnostics, with over 30 million investigations per year using the isotope. Since most ^{99}Mo production is done in nuclear reactors with ages of over 40 years, research is done to find alternative methods of ^{99}Mo production not reliant on these aging reactors. Currently, the most used method to produce ^{99}Mo is to irradiate solid targets with Uranium-235 with neutrons coming from a reactor core. This work investigates a variation of this production method using an uranium salt dissolved in water inside an U-shaped tube located within a tube near a reactor core. This U-tube is irradiated with neutrons coming from the 'Hoger Onderwijs Reactor' (HOR) at the TU Delft reactor institute.

Using Matlab and Serpent, a model was made to simulate a loop of uranium salt flowing inside the HOR. Simulations were done to investigate and optimise the production capacity of medical isotopes using this uranium salt method. The parameters investigated to assess the optimal production capacity were the U-tube orientation, the material surrounding the U-tube, the choice of uranium salt as well as its concentration and the salt's flow speed . It was found that a 3-hour irradiation cycle was optimal for the salt, leading to a weekly ^{99}Mo production of 290 6-day Curie. Assessments were also made on the safety of this type of medical isotope production. It was found that leaks of either uranium salt or water can be detected in the isotope output concentration, but hardly in the multiplication factor of the system since the changes in multiplication factor caused by these leaks are within several standard deviations of the k-factor value without a leak. A temperature profile of the salt solution in the tube was also made by looking at the amount of ^{235}U fissions that occurred during a single time step. It was found that the temperature increase in the salt was manageable and would decrease in case of leaks.

Table of Contents

1. Introduction

This thesis discusses the feasibility of producing the medical isotope Molybdenum-99 (^{99}Mo) in a loop close to the core of the 'Hoger onderwijs reactor', the research reactor at the TU Delft. An uranium salt dissolved in water is assessed as the target for neutron irradiation. ^{99}Mo is an important medical isotope since its daughter isotope ^{99m}Tc is used in over 80% of medical imaging, entailing over 30 million investigations per year. Since the dependence on these isotopes is high and since the structures creating them are rather old, disruptions in the supply chain are a real threat that can lead to worldwide isotope shortages. As recently as between 2008 and 2010, a worldwide supply crisis already occurred because of multiple reactors having unexpected downtime. To combat these shortages and prevent future crises, it is useful to increase the amount of production sites for this isotope by letting smaller research reactors create isotopes to fulfil local needs. The point of this thesis is therefore investigating the potential of turning the Delft research reactor in one of these smaller suppliers using uranium salts in an U-tube which are irradiated by the reactor core.

1.1. Nuclear reactors and fission

Nuclear reactors work on the principle of splitting heavy nuclei, such as for example Uranium-235 (^{235}U), into two fragments after interaction with a neutron. This split releases not only these two fragments, but also new neutrons and energy. The new neutrons can be used to cause new fissions, leading to a fission chain reaction as can be seen in figure 1.

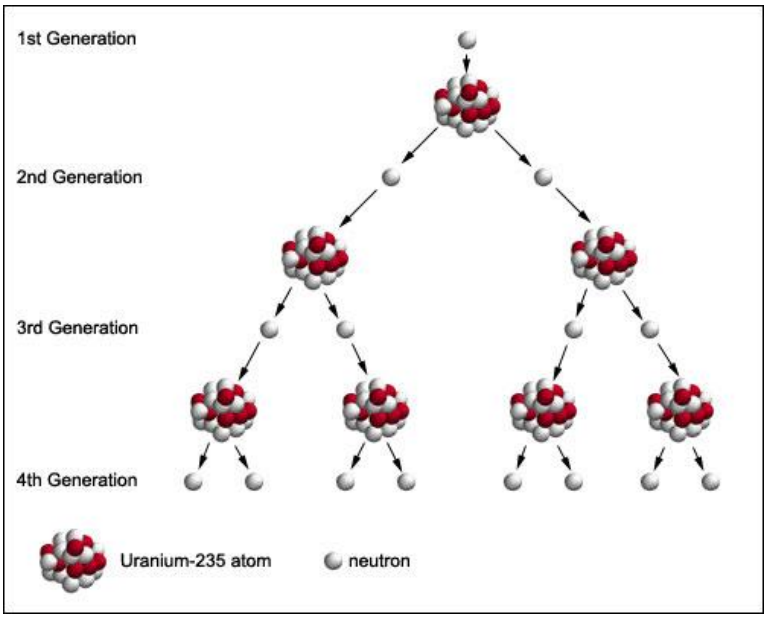

Figure 1 Fission chain reaction[1]

It should be noted that in nature, pure ^{235}U does not exit. Natural uranium consists mostly of ^{238}U with only small percentages of Uranium-234 and Uranium-235. Because of this, uranium is enriched in ^{235}U . Enrichment refers to the process of increasing the mass percentage of ^{235}U.

The multiplication factor or k-factor of a nuclear process describes how this chain reaction develops. For example, imagine fission chain reaction where every neutron causes a fission that supplies the system with two new neutrons. If these two new neutrons both also causes fission, the multiplication factor of such a process is 2. On average 2,5 neutrons are supplied per ^{235}U fission reaction. This leads to a nuclear chain reaction, where every fission event leads to new fission events, making a chain of fissions that is self-sustaining. A chain reaction as simple as the one in the example is generally not realistic though. Neutrons will not always react with an ^{235}U nucleus and could just leak away from the reactor or interact with another nucleus leading to a lower k-factor. Not every neutron released is guaranteed to react with the desired fissile nucleus.

The microscopic cross section of a nucleus is a concept that is used to describe nuclear fission. It is used to represent the probability of a neutron nucleus interaction. Given an uniform beam of

neutrons with an intensity I in cm^{-2} s^{-1} which strikes a one atom thick layer of atoms with N_a atoms cm^{-2}, the number of interactions per cm^2 per second C can be defined as:

$$C = \sigma N_a I \tag{1.1}$$

Here, the σ is the so microscopic cross section. It is a proportionality factor for interaction and its unit is cm^2. The unit that is usually used for the microscopic cross section however is the barn. A barn is a unit in physics equivalent to 10^{24} cm^2. One can consider σ to be the effective 'target area' that a nucleus presents to the neutron.[2,3] Going from one nucleus to the entire material, one has to simply multiply the microscopic cross section for an individual nucleus with the atomic density N in the material to get the macroscopic cross section.

$$\Sigma = \sigma N \tag{1.2}$$

Seeing as N is the number of atoms per cm^3, Σ has the unit cm^{-1}. The probability that a neutron travels a distance x in a material without interaction is then given by:

$$P(x) = e^{-\Sigma x} \tag{1.3}$$

In the case that a material consists of multiple different kinds of nuclei, the macroscopic cross section of this material can be calculated using:

$$\Sigma = \sum_i \sigma_i N_i \tag{1.4}$$

For a safe and well-functioning reactor, the amount of energy produced has to be stationary, meaning the k-factor has to be 1. A system with a k-factor of 1 is referred to as a critical system, with a k-factor of above or below 1 being respectively supercritical and subcritical.

A light water reactor is made up of fuel rods, containing a fissile material that includes for example ^{235}U, assembled into a lattice structure and surrounded by coolant. The coolant is used to absorb the heat produced by the fission, often with the purpose of using this absorbed heat elsewhere to produce electricity. Water is most commonly used as a coolant. Another common use for water is moderation. A moderator is a substance, often water or graphite, that slows the neutrons created in a fission. This is because the chance of a fission occurring is dependent on the speed of the incoming neutron and for some nuclei a slowed down neutron has a higher chance of causing fission. In the case of ^{235}U for example, the neutrons created in fission are too fast and slowing them down significantly increases the amount of reactions that occur.

The fuel rods are housed in a metal cladding, the chosen metal has to have few neutron interactions and therefore metals such as zirconium and stainless steel are used. This cladding is used to separate the fuel from the coolant to prevent any chemical reactions between the two and to ensure that no radioactive material can be spread throughout the reactor by the coolant.

Other important parts of a nuclear reactor are the control rods and the reflector. The control rods are made of a material that absorbs a lot of neutrons without fission occurring. These rods are placed in a reactor to control the amount of neutrons that is available for further chain reactions to ensure

that k stays at 1 or to completely shut the process down if needed. The reflector is a material that reduces neutron leakage from a reactor by reflecting neutrons that would have leaked back into the reactor. A material that is often used for reflectors is beryllium.[2,3]

1.2. Hoger Onderwijs Reactor

The 'Hoger Onderwijs Reactor' (HOR) is an open pool-type research reactor located in Delft. The HOR has a core consisting of twenty lowly enriched uranium, which is uranium fuel with an ^{235}U mass percentage of 20% or less, fuel rods[4] and reflectors made of beryllium. It generates around 2MW of power. It is primarily used as a neutron source for experiments done at the Reactor Institute Delft. Figure 2 shows a picture of the HOR's core. In this thesis, the potential of ^{99}Mo production using the HOR will be assessed. The method of ^{99}Mo production studied is that of uranium salt solution irradiation. An U-tube is to be placed in a vertical tube near the reactor core. This U-tube is then filled with an uranium salt that is dissolved in water, which will then be irradiated by neutrons coming from the reactor core. This leads to a fission chain reaction and ^{99}Mo production because of the fission of ^{235}U within the uranium salt, since this fission can result in ^{99}Mo. Figure 3 shows a shematic representation of this U-tube inside the outer tube. Figure 4 shows a schematic upper view of the HOR's reactor. The 'outer tube' mentioned in figure 3 is the tube to the right of the core in this figure.

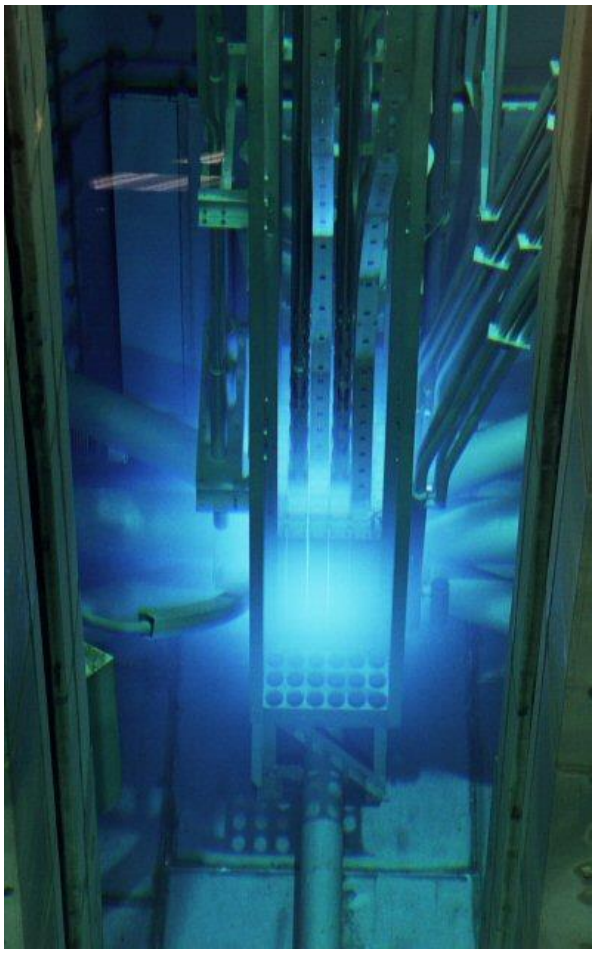

Figure 2 A picture of the HOR's reactor core[4]

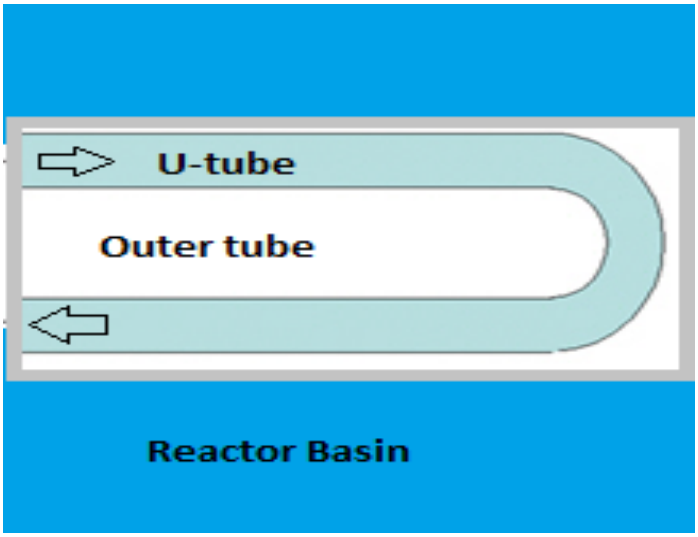

Figure 3 A schematic representation of the U-tube filled with uranium salt

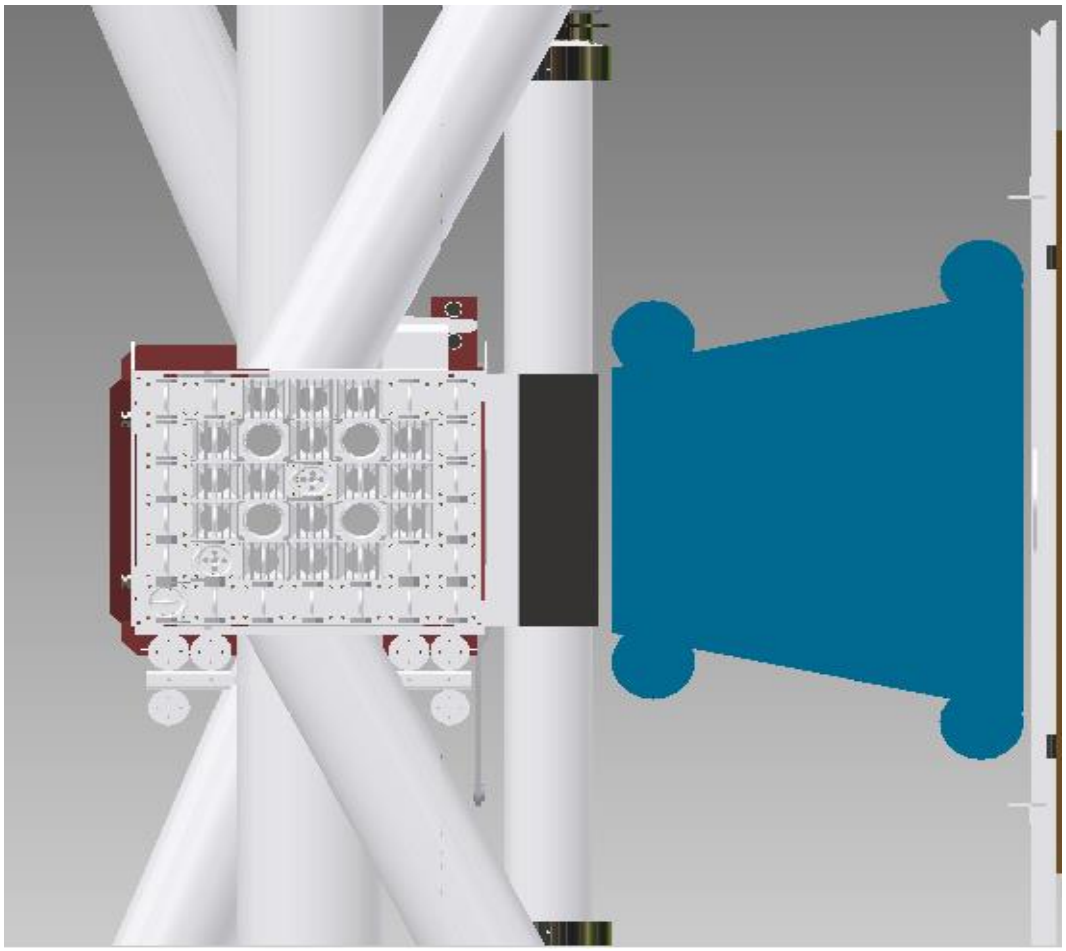

Figure 4 A schematic upper view of the HOR's reactor

1.3. The worldwide $^{99}Mo/^{99m}Tc$ supply chain

^{99}Mo is mostly produced by fission of ^{235}U targets. In 6.1% of ^{235}U fission reactions, ^{99}Mo or a parent isotope that quickly decays into ^{99}Mo is produced alongside multiple (generally two) neutrons, additional isotopes such as Iodine-134 and Tellurium-134 and energy. Producing the isotope is however only the first step in the chain of processing these isotopes for medical use. The full supply chain can be seen in figure 5.

Figure 5 The ^{99}Mo supply chain[5]

The supply chain starts with the production of uranium targets for irradiation. The choice of enrichment and composition of these targets will be discussed later. After creation these targets are sent to an irradiation facility, where they will undergo irradiation. This is done by placing the uranium targets near the reactor core, which means neutrons that leave the core are likely to irradiate the targets. The irradiation of targets takes between 6 and 7 days[6] using conventional production

methods. Once the targets are done with irradiation, they are cooled and prepared for shipping. This process takes around 16 hours in total. [6] To make sure as little of the medical isotopes is lost as possible, it is required that a production facility is no further than 1000 km from an extraction facility. This means transport is generally not supposed to take longer than a couple of hours. Once at the processing facility, ^{99}Mo is separated from the rest of the isotopes in the targets, resulting in ^{99}Mo bulk liquid. This separation process takes around 12 hours. [6] This bulk liquid is then transported to a generator manufacturing facility, this transport can take up to 36 hours depending on the location of the extraction and generator plants. [6] At the generator plants, the bulk liquid is used to produce ^{99}Mo/^{99m}Tc generators by absorbing the ^{99}Mo to an alumina column and placing this column inside a generator. Preparation of these generators can take up to a day and transport of these generators to hospitals also takes up to a day. [6] Once at the hospital, radio pharmacists can use the generators to prepare the required dose of ^{99m}Tc for whatever imaging the patient needs using a so called 'cold-kit' and a saline solution to remove ^{99}Mo from the generator column. Once at a hospital, a generator can be used for around two weeks before a new one is needed.[6]

As is evident from the description given above, one of the vital aspects of this supply chain is speed. This is because ^{99}Mo has a short half-life of 66 hours and ^{99m}Tc has a half-life of only 6 hours. A quick supply chain is needed to minimise the amount of isotopes that is lost before the product is ready for usage.

Because the time between the end of irradiation at a reactor facility and the isotopes being in a useful state at a hospital is about 6 days, the unit used when talking about ^{99}Mo production is the 6-day Curie. The Curie itself is an unit for radioactive activity defined as:

$$1Ci = 3.7 \times 10^{10}\ Bq \tag{1.5}$$

So 1 Curie is equal to 3.7×10^{10} decays per second. The 6-day prefix means that one looks at the activity 6 days after production. Given the ^{99}Mo half-life of 66 hours, this means that the activity in 6 days is only 22% of the activity directly after irradiation.

There is a weekly worldwide demand of ^{99}Mo of around 12000 6-day Curie.[6] Most of this demand is met by a small number of large reactors all of which are also quite old, with most of them being constructed around the 1960's. Main reason for supply crises are emergency maintenance and unexpected shutdown for safety reasons. The amount of unexpected downtime these plants will have will only increase with the age of these plants. The main reason these isotopes are still being produced in old reactors is that ^{99}Mo production is currently not economically viable for new reactors. This is because originally the production of these isotopes was seen as a by-product of normal reactor operations and therefore the ^{99}Mo was priced as such[6]. This means that the cost of creating and running a new, isotope-production reactor cannot be met by the low sales price of ^{99}Mo alone, requiring for example government support to keep the reactor running. These complications and need for outside help have limited the initiatives for new large scale isotope irradiation facilities and has therefore led to smaller scale projects where some ^{99}Mo is produced for local consumption.

1.4. Current techniques for ^{99}Mo production

There are currently two techniques that are used for the production of ^{99}Mo, i.e. accelerator based ^{98}Mo neutron capture and fission of ^{235}U. The usage of ^{98}Mo for ^{99}Mo production is currently only used in small scale facilities in Kazakhstan and Romania. Because of the low specific activity of ^{99}Mo produced by this process (~1 Ci/g), as well as the lower cross section for ^{99}Mo production compared to fission, this technique is not suited for large scale production.[7,8]
^{235}U fission is the main method of ^{99}Mo production. As stated earlier, uranium targets are placed

inside a reactor where they are irradiated by the neutrons coming from these reactors. Fission takes place in these targets and 6.1% of the fission reactions lead to ^{99}Mo. ^{99}Mo produced by this method has a high specific activity (~10^4 Ci/g)[8]. The targets used in this process are currently highly enriched uranium (HEU) targets. HEU targets have an uranium enrichment of more than 20% and generally up to 95%. This is one of the major concerns with this method of ^{99}Mo production, HEU is enriched up to weapons grade proportions and therefore transport of targets has to be highly secured and controlled.

Five facilities supply the world with ^{99}Mo using HEU targets. Production specifics of these facilities are listed in table 1.

Table 1 A listing of all major ^{99}Mo producers[9,10]

Country/Location	Name	Thermal Power, MW	Maximum Yearly Operation Days	Typical share of world production
Netherlands, Petten	HFR	45	290	30%
Belgium, Mol	BR-2	100	115	10-15%
Canada, Chalk River	NRU	135	315	40%
France, Saclay	OSIRIS	70	220	5-8%
South Africa, Pelindaba	SAFARI-1	20	315	10-15%

To remove the problems inherent to the usage of HEU, targets have been developed made with lowly enriched uranium (LEU). This is far below weapons grade and thus security requirements would be lower when using LEU. LEU is already used on a relatively large scale in Argentina and Australia amongst others, where between 1 to 5% of the global ^{99}Mo need can be produced.[7]

LEU targets are generally comparable to HEU. Irradiation of LEU targets takes around 6 days[11] on average, just as with HEU targets, and the same ^{99}Mo extraction methods can be used. There are some notable differences between the two sorts of targets however. Firstly, LEU targets need about 5 times more total uranium mass than HEU targets to have equivalent yields. In other words, the amount of ^{235}U in LEU targets has to be about the same as the amount in HEU. To this effect, a large mass of LEU is put into the targets with the goal to have an ^{235}U mass equivalent to that of a standard HEU target. Because of this, the amount of targets that need to be irradiated will be about the same for both[12]. Secondly, LEU targets are much simpler to acquire, since more fuel manufacturers have access to LEU as opposed to HEU, which only a couple of specific companies and labs have access to.[12] Thirdly, because of the increase in uranium mass in the targets, the amount of uranium waste that originates from ^{99}Mo production will also increase[7]. The amount of ^{239}Pu waste is also increased, because of the increase in ^{238}U in the targets, by a factor of approximately 25[7]. However, the total amount of liquid waste stays about the same. This is because LEU need less liquid to dissolve in, keeping total liquid waste volumes unchanged.[12] It should also be noted that ^{239}Pu could also be used for ^{99}Mo production and is therefore technically not waste. ^{239}Pu is however never really used for isotope production since targets using ^{239}Pu have never been developed and doing so would as of yet not be worth the cost.[13]
The quality of ^{99}Mo produced with LEU is equal to that of HEU ^{99}Mo[12]. The α-contamination (measure for the amount of unwanted α particles radiating from the solution) of ^{99}Mo produced by LEU is about 20% higher than that of HEU. This α-contamination exists because even after purification of ^{99}Mo, some unwanted isotopes will remain and some of these isotopes sadly emit α-particles. The reason for this difference in the amount of contamination is that while LEU has more ^{239}Pu in it, which causes about half of the α-contamination of LEU, HEU has a higher enrichment. This high enrichment leads to a higher percentage of ^{234}U, which is also a large source of α-contamination.

These two different contamination sources compensate for each other, leading to the small difference in purity. ^{99}Mo from LEU targets also has the same high specific activity that isotopes from HEU targets have.[12]

The main problem for LEU is currently that it is not economically viable to convert the current irradiation reactors for LEU and neither is making new reactors that have LEU based ^{99}Mo production in mind. On top of this, current reactors are too old to convert, meaning LEU production capabilities would not be worth it since the reactor itself still has to be replaced.

LEU targets will be used as the main comparison for the salt solution based ^{99}Mo production investigated in this thesis. This is because both methods use LEU and because in both cases the uranium is irradiated with neutrons from a reactor core. Since as mentioned above, HEU targets and LEU targets are generally comparable, data for HEU targets can also be used if LEU data is insufficient.

1.5. Current techniques for ^{99}Mo extraction from bulk liquid

There are a total of 4 large plants where ^{99}Mo is separated from ^{235}U targets. These extraction facilities are listed in table 2. The share percentages in this table add up to 99%, the last percent is supplied by some minor production and extraction plants which mainly supply their domestic market. Argentina and Australia for example are both countries that have such a smaller scale ^{99}Mo sources. The smaller extraction facilities generally have some room to grow and can potentially become minor exporters of ^{99}Mo bulk liquid.[6,14]

There is one exception to the general operations of extraction facilities. Nordion in Canada does not extract the ^{99}Mo from the initial ^{235}U solution. The extraction is done at the irradiation site itself, but it is not possible at this plant to purify the bulk liquid sufficiently for medical use .Therefore, it is sent to Nordion for purification.[6]

Table 2 A listing of all major ^{99}Mo extraction facilities[6]

Country/Location	Name	Supplied by	Processing capacity, 6-day Curie per week	Typical share of world supply
Netherlands, Petten	Covidien	HFD, BR-2	3500	30%
Belgium, Fleurus	Institute for RadioElements	BR-2, OSIRIS	3000	12%
Canada, Ottawa	MDS Nordion	NRU	7200	39%
South Africa, Pelindaba	NTP Radioisotopes	SAFARI-1	3000	18%

As is evident from this table, the amount of ^{99}Mo actually processed by these facilities is lower than their actual weekly capacity. Processing capacity is generally higher than actual used volume because the plants need to have a certain amount of reserve capacity. Plants have reserve capacity because they need to have a backup in case of shutdown or unscheduled outages as well as to account for operational realities of research reactors.[6] All productions plants mentioned in paragraph 1.4 supply ^{99}Mo to the geographically closest extraction plant. As has been explained earlier, ^{99}Mo has a half-life of 66 hours so the time between irradiation and processing has to be minimised. This also means that if one processing facility has to be shut down, irradiation plants in its area will effectively

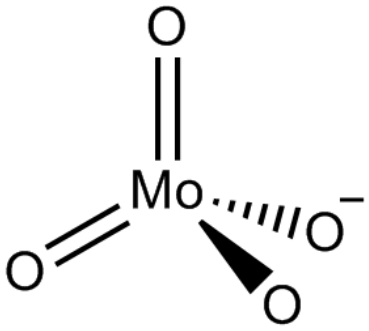

Figure 6 Molybdate (MoO_4^{2-}) [15]

produce less ^{99}Mo because their targets have to be transported a larger distance.

^{99}Mo is extracted from the targets at these facilities using separation columns. To this effect the solid HEU and LEU targets that are generally used need to be dissolved first. The classic sorbent used for ^{99}Mo extraction has been alumina, since most of the ^{99}Mo in the solution exists as the negatively charged compound molybdate.[16,17] Molybdate effectively binds to the alumina and because of this interaction, ^{99}Mo in its molybdate form can be separated from the solution using separation columns. Experiments have been done to test the effectiveness of other sorbents and three specific sorbents, called radsorb, isosorb and PZC, were specifically tested to be used as a sorbent for the uranium salts uranyl nitrate and sulphate solutions.[16] The reason for this is that classic alumina sorbent is less effective for these uranium salts than it is for the dissolved uranium targets. This makes alumina a bad option for ^{99}Mo extraction using uranium salt based methods such as the one researched in this thesis. Because of this, these alternative sorbents will be considered for ^{99}Mo production with the HOR. The reason alumina is a less effective sorbent for uranyl nitrate and sulphate is that the ions from the sulphate and nitrate compete with the anion molybdate for binding to the alumina. Figure 7 shows the difference in absorption quality between these three sorbents and alumina. As can be seen, they outperform alumina for every uranium concentration in an uranium salt. The unit on the y-axis of figure 4 is the so called distribution coefficient K_d defined as:

$$K_d = \frac{\left(\frac{A_o - A_s}{W}\right)}{\frac{A_s}{V}} \tag{1.6}$$

Where A_o and A_s are respectively the aqueous phase activity before and after equilibrium in counts per minute (cpm), W is the dry weight of the sorbent in g and V is the aqueous phase volume in mL. Since these three sorbent significantly outperform alumina in extraction from uranium salts, they will be the sorbent used when extraction capabilities are considered.

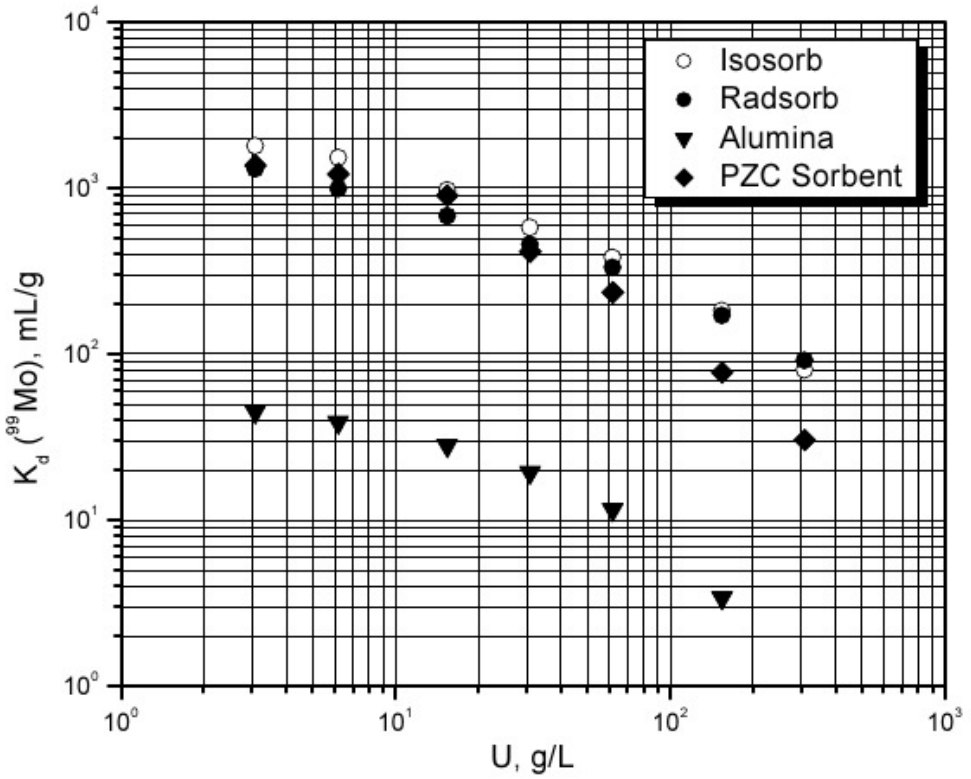

Figure 7 Absorption quality for different sorbents given uranium concentration[16]

1.6. Possible usage of uranium salts dissolved in water in ^{99}Mo production

Aqueous homogenous reactors(AHR) are a type of ^{99}Mo production reactor. They are based on the concept of using an uranium salt dissolved in water to produce medical isotopes. An AHR consists of an enriched uranium salt dissolved in water and acid inside a shielded tank. This means the fuel (uranium salt), coolant(water) and moderator(water) are homogenously spread throughout the vessel. The enriched uranium salt can be both HEU or LEU, but LEU is the more commonly used variant. Because the liquid inside the reactor vessel is a mix of both moderator and fuel, simply increasing the amount of fuel will not always lead to an increased isotope production. Adding more uranium salt means that the amount of water in the solution is lower, which lowers the total amount of moderation and since this moderation is needed for ^{235}U fission, total isotope production can in fact decrease with increased uranium concentrations.[16,18]

Even though interest in AHRs has recently increased because of their potential as an alternative for classic ^{99}Mo production, the concept of AHRs themselves is older. The first AHRs were built in the 1940's to study things like fission cross sections and to make critical mass calculations for different isotopes. The idea of using an AHR for isotope production was proposed in the 1992 to supply the growing demand for medical isotopes around the world.[18]

One has to be aware of the fact that the production method researched in this thesis and an AHR are not equivalent, even though both use an uranium salt for ^{99}Mo production. This is because in an AHR, the dissolved salt is also the main fuel that keeps up the nuclear chain reaction, while in the method used in this thesis the salt is irradiated by an outside source, i.e. the reactor core. For this reason, this method is more comparable to ^{99}Mo production by irradiation of LEU targets as was previously stated.

1.7. Goal and Outline

Goal

The goal of this thesis is to assess the feasibility of producing ^{99}Mo in the HOR using an uranium salt in an U-tube that is irradiated by neutrons from the reactor core. Furthermore, this production capacity will be optimised with regards to inlet flow salt concentration, U-tube positioning and in-tube material choice. All of this is to be done using the Monte Carlo reactor physics code Serpent.

Outline

In order to make this assessment, chapter 2 gives an explanation of the codes and models used for this simulation. The main processes within the Serpent code will be explained and the relevant input parameters will be discussed. Based on this data, the full simulation process as it was used for this thesis will be explained.

Chapter 3 presents the results of the different simulations done, as well as an assessment of the safety of the proposed system.

Chapter 4 gives the conclusions, as well as suggestions for further research based on the findings of this report.

The appendix will feature a detailed description of Serpent, the Monte Carlo simulation code used for this thesis, as well as exact descriptions of the input parameters used in the simulation.

2. Codes and Models

To investigate whether or not ^{99}Mo production is viable in this reactor, a simulation of reactor and the U-tube filled with uranium salt will be made in Serpent, a Monte Carlo method based reactor physics simulation code that will be discussed in paragraph 2.1. The geometry of most of the reactor will be discussed in paragraph 2.2. The geometry inside the tube that will be used for isotope production, as can be seen in figure 3, is flexible and it will therefore be optimised by looking at the maximum isotope production that can be achieved by variation of U-tube orientation and inner tube filling. This will be discussed in both the chapter 2.2 as well as chapter 3. The salt to be used for production is also a parameter that has to be chosen with an eye on optimal production ^{99}Mo production. The selected salt will be discussed in paragraph 2.4, while the optimal concentration of this salt solution will be researched and discussed in the results. Serpent, the Monte Carlo reactor physics burnup calculation code used for this simulation, needs a reactor geometry input and material definitions for both the salt and the reactor components to function. Serpent will be discussed in paragraph 2.1 and appendix A. On top of Serpent, Matlab was used to process Serpent's output data and create new input data for Serpent. The full simulation process using both Serpent and Matlab will be discussed in paragraph 2.3.

2.1. Serpent

The Monte Carlo method is best described as a brute force calculation technique that solves problems by simulating large amount of specific solutions to a problem. Unlike normal simulations, where all input variables have a fixed value, Monte Carlo simulations have input values which have a probability distributions. By doing a large number of simulations, each with their own starting conditions sampled from the input values with specific probability distributions, one is able to generate a final output based on all individual simulations. This output will therefore also be stochastic and have a specific probability distribution, which will have a mean and a standard deviation. One important term in the context of random number generation is the seed. The seed is a number used to initialize the random number generator in a stochastic simulation. Using the same seed for different simulations leads to the same random numbers being generated for both simulations. Because of this, different set ups can be compared.

The input values with a probability distribution in the case of reactor physics are variables such as the parent isotope location and the isotope and type of reaction from which the neutron originates . Neutrons are simulated one by one with every neutron having random energy and movement generated from the probability distribution. The total of these generated neutron parameters are then used to follow the life of the individual neutron within a geometry set up by the user. Based on the simulated movement of a neutron, Serpent calculates the interactions this neutron would undergo. By doing this for a large number of neutrons, Serpent derives a distribution for neutron interaction within the geometry defined by the user. The simulation of these individual neutrons is referred to as neutron tracking. A neutron track in this context is the shortest path between two points of neutron interaction, these points can be interactions like transition from one material to the next, so for example transition from a reactor core to the water inside a reactor bath, or a scattering of the neutron with a nuclide inside the material. The combination of all these individual tracks, from emission to the final interaction, form a neutron history and the combination of neutron histories then forms a model for the reactor neutronics.[19]

The full process of Serpent simulation is visible in figure 8. All individual parts of the simulation process are discussed in appendix A. But the main principle is that things like initial energy and direction are sampled from a random distribution, then used as input parameters for the simulation, which allows the simulation to determine where and how a neutron interacts. By doing this in a cyclical fashion for a large number of neutrons per cycle, Serpent calculates neutron distributions and interactions within the simulation.

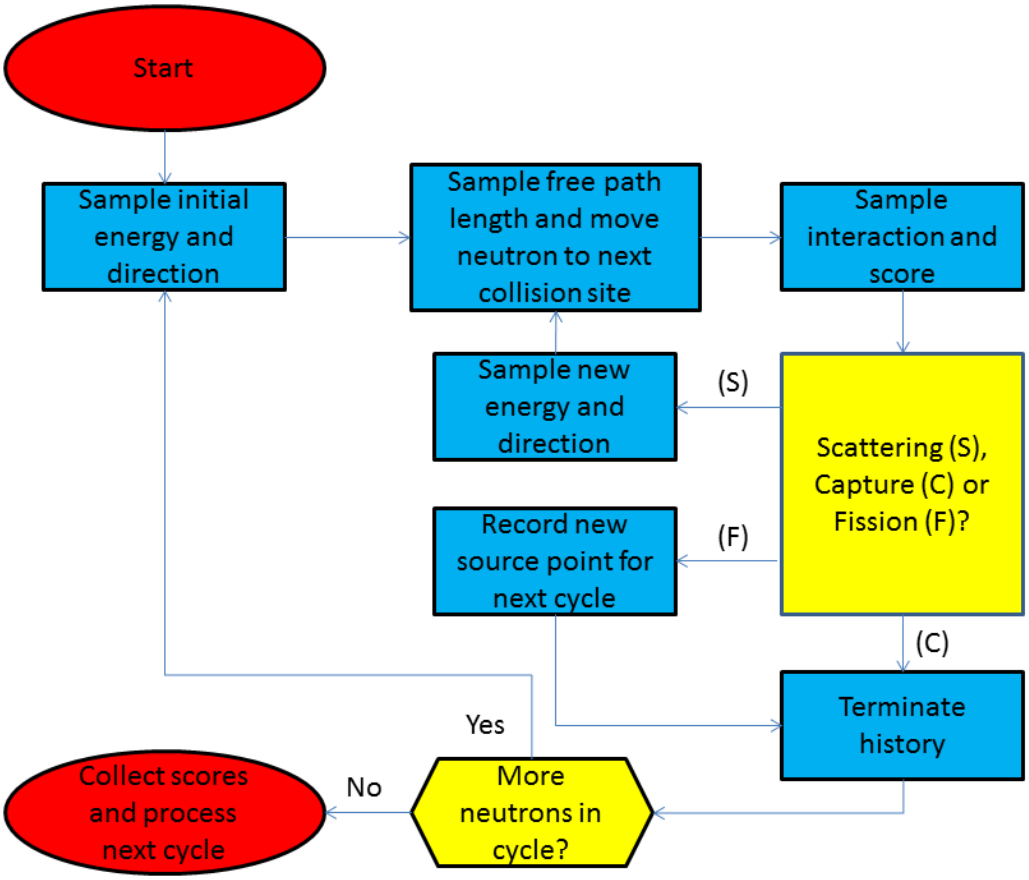

Figure 8 Schematic representation of Serpent simulation process

2.2. Reactor Geometry

In order for Serpent to work, a clear reactor geometry has to be defined. Figures 9 shows the relevant geometry section of the RID research reactor from a sideways perspective. This is the same geometry that was shown in figure 4.

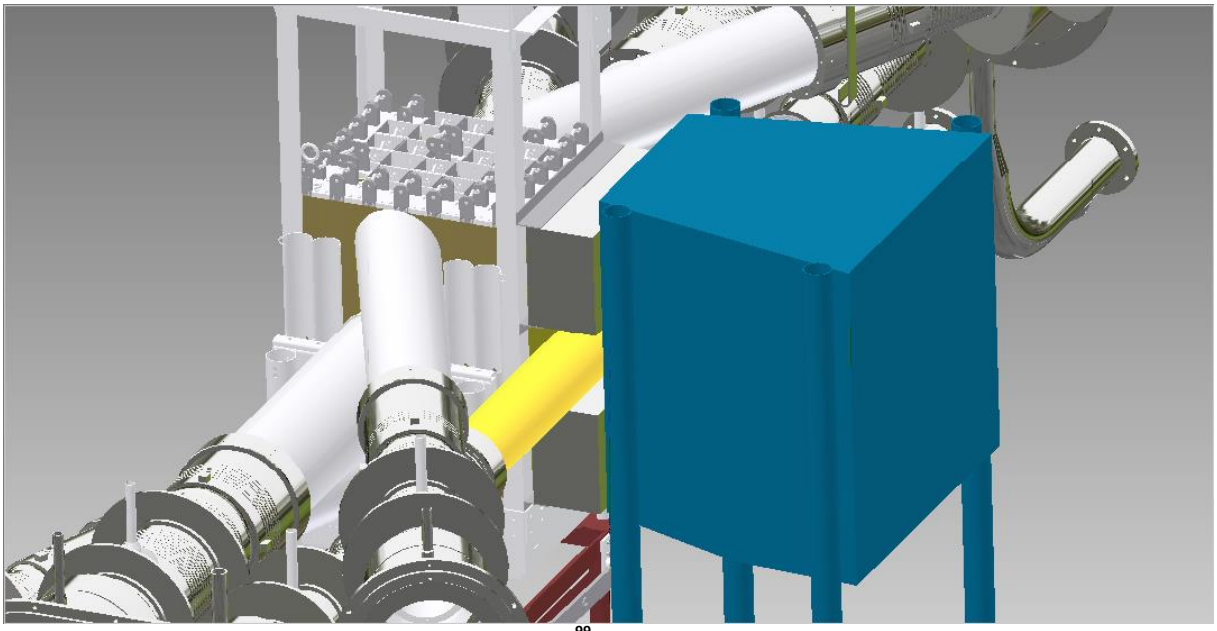

Figure 9 Sideways view of reactor geometry and the ^{99}Mo facility

The tube in which ^{99}Mo is to be created is highlighted in yellow in figure 9. The yellow tube is this outer tube mentioned in figure 3. The U-tube with uranium salt in it is to be placed inside this yellow tube. The U-tube is made to be as large as it can be within the outer tube, with a bit of room between the outer tube and the U-tube to make sure the U-tube can be placed and positioned inside the system. The exact composition of this tube and all other aluminium tubes in the reactor can be found in appendix B. The simulated U-tube consist of two cylinders with an inner radius of 3.1 cm and an outer radius of 3.3 cm with their centres at a distance of 8 cm from each other, within the outer tube which has an inner radius of 7.5 cm. Since two cylinders are used for the U-tube, the joint is not simulated. This is done because Serpent does not support shapes like an U-tube. Since the joint is at the end of the tube, the irradiation at this point should be lower than that at the centre of the tube near the core which is accurately simulated. This means the joint can be simplified like this, since the main irradiation is still accurately simulated.

To model the reactor efficiently, simplification have been made to the geometry as it can be seen in these images. First of all, the aluminium tubes at the sides of the reactor, which work as neutron windows for other experiments, are not simulated, since these tubes are relatively far from the U-tube filled with the salt solution and as such their presence should not really influence the salt production. By leaving these tubes out of the simulation, the system becomes significantly simpler, leading to less memory needed to store all the parts of the geometry and thus to a faster simulation time. Secondly, the reservoir behind the salt tube, which is blue in these images, was edited. This trapezoidal reservoir is the so called nitrogen reservoir. This nitrogen reservoir is an aluminium box, generally filled with water, that is occasionally filled with nitrogen for specific experiments. Because of its shape simulating this structure is computationally intensive. This is because Serpent is only capable of simulating cubes, spheres, cylindrical shapes and planes. So in order to create a trapezoidal structure, a large amount of cuboids have to be placed in order to simulate the structure of a trapezoid. This is computationally intensive and should therefore be avoided. To counteract this effect, two different alternative geometries will be tested next to the accurate model with the full

trapezoidal. These two are the simplified model (which will be called simple for short), where the trapezoid is replaced with a cube of comparable size, and the short model, where only a couple of centimetres of the trapezoid is simulated after which points the simulation is stopped. The idea behind the short model is that neutrons will generally not get much farther than a couple of centimetres into the water filled nitrogen reservoir before interacting in some way, since the expected diffusion length is 10 centimetres at a maximum. Therefore simulating the entire shape is unnecessary. Figures 10 until 14 show respectively an XZ perspective, an YZ perspective, the XY perspective of the accurate model, the XY perspective of the simplified model and the XY perspective of the short model.

The core is simulated in a simplified fashion, using homogenised blocks of fissile material and reflectors in a lattice structure. As can be seen in figures 8 until 12 the core is made up of 42 blocks in total, 20 of which are made up of fissile material and 22 of which are reflector elements. The size of the fuel blocks is 7.71 by 8.1 by 60. They are made up of a combination of 38 radioactive isotopes combined with aluminium and water, all of it completely homogenised over the block. The other blocks in the core are the beryllium reflectors. These reflectors are slightly smaller than the fuel blocks, with a size of 7.7 by 8.0 by 60. The space not filled by beryllium in the reflectors blocks is filled with water so that these blocks are also 7.71 by 8.1 by 60 in size. The initial homogenized block data created a system that was significantly sub-critical at a k-factor of around 0.7. To compensate for this, the homogenised blocks used in the core were changed and blocks that had low atomic densities of ^{235}U were replaced with blocks with higher densities until the k-factor of the system was 1, as it should be for the RID reactor. The initial homogenised blocks can be found in appendix C. The adjusted core with a k of 1 that was used for the simulation can be made from this core by replacing blocks 11 until 20 with block 6, which is the block with the highest ^{235}U density. The power of this system is normalised to the 2 MW that the reactor normally produces. The above means the power is being underestimated, since the production inside the salt solution is not being considered. This normalisation is necessary however for the simulation to work since the burnup calculation requires a normalised amount of power to calculate isotope production properly. Since the power output of the salt should be significantly lower than that of the reactor given the higher activity in the reactor and its k-factor of 1, this underestimation does not have a significant effect on the accuracy of the simulation.

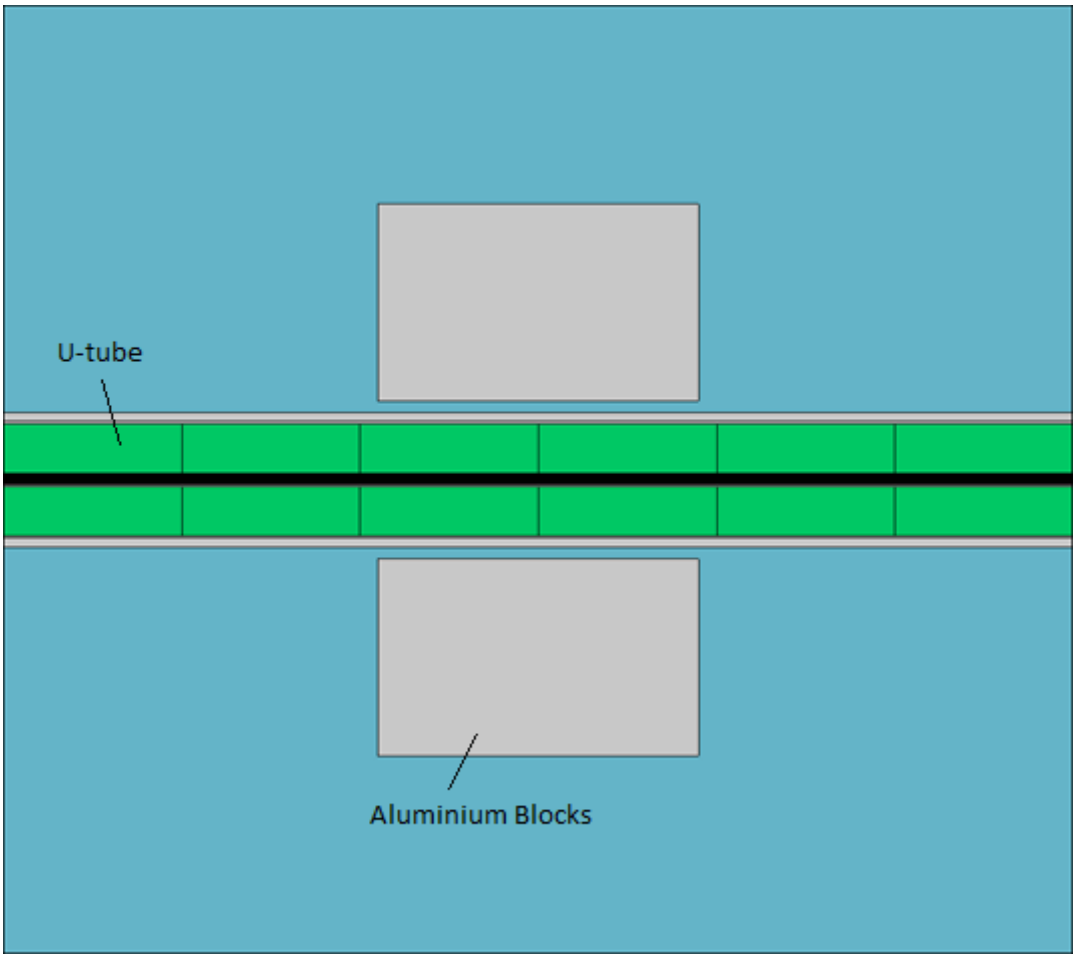

Figure 10 XZ perspective of reactor geometry in Serpent

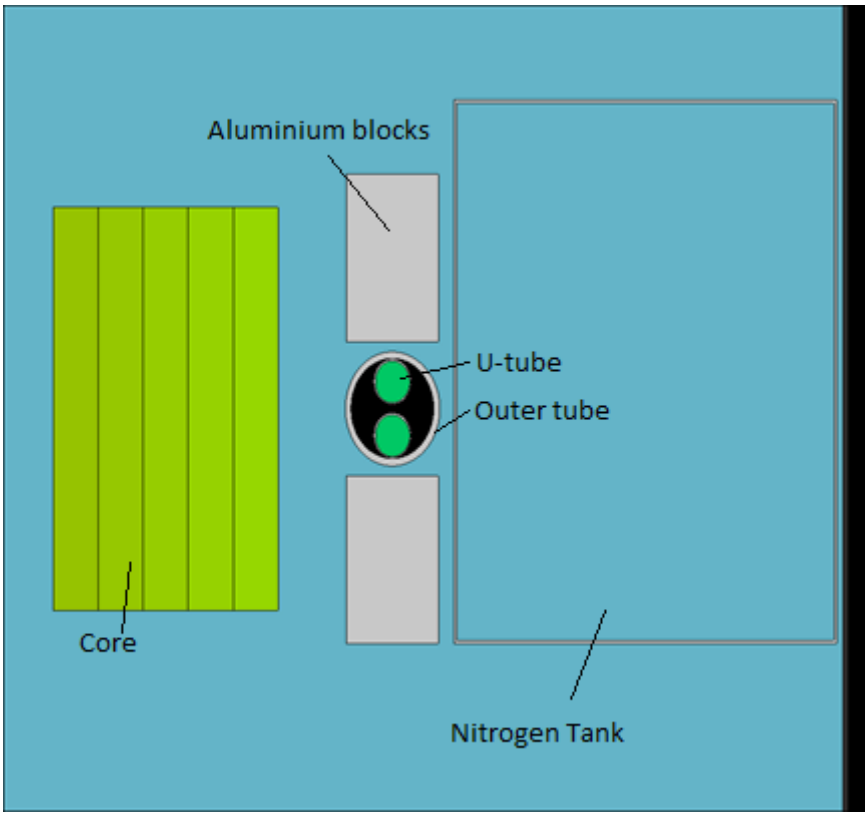

Figure 11 YZ perspective of reactor geometry in Serpent

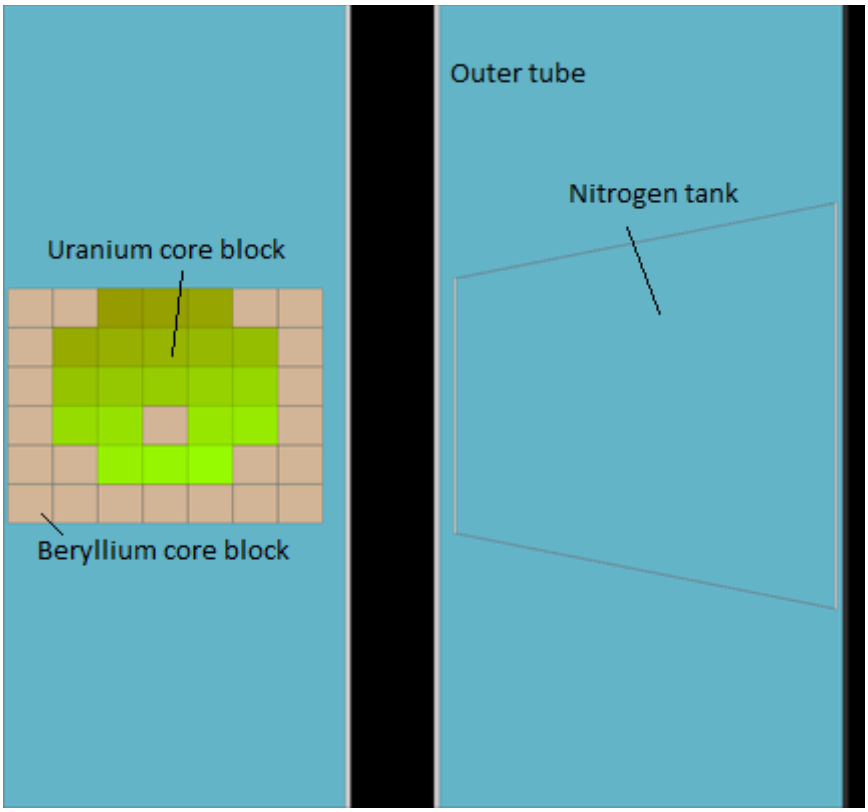

Figure 12 XY perspective of accurate reactor geometry in Serpent

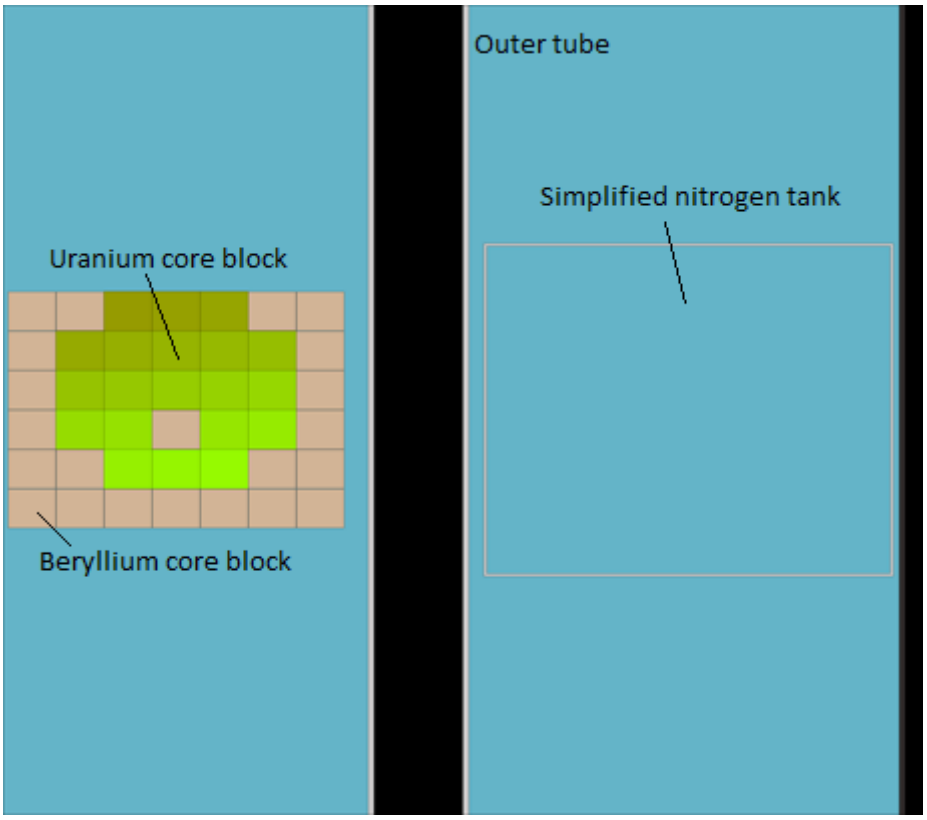

Figure 13 XY perspective of simple reactor geometry in Serpent

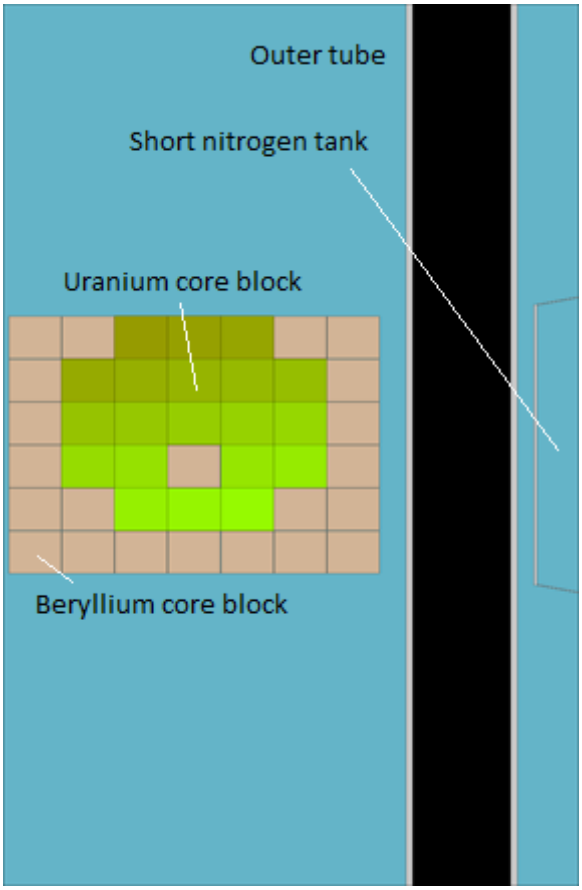

Figure 14 XY perspective of short reactor geometry in Serpent

2.3. Simulation process

The complete process that was used for the simulations is depicted in figure 15. An important thing to note is that for this simulation the salt solution in the U-tube is separated into 12 sections. The reason for this it that the salt solution in these sections can then be moved to the next section in Matlab to simulate the convection of the solution. The choice for 12 segments is a compromise between accuracy and computational time. It is obvious that the more sections the system has, the more accurate the calculation becomes. However, every section needs some calculation time in Serpent for the burnup calculation so more sections would mean a higher calculation time. This is because every section is calculated individually, which means that an increase in sections is an increase in the number of individual calculations that has to be done. Secondly, since the simulation starts with non-irradiated salt solution in the entire tube, the simulation has to run a number of cycles equal to the number of sections before a steady state situation is reached. This is because all cycles before then have a salt solution in the outflow that has not undergone full irradiation, but has instead only partly been irradiated before leaving the system. Since a step can be anywhere between 5 and 45 minutes it is important to limit the amount of steps and therefore the amount of segments. Using 12 segments and 15 steps computation time can be kept at a manageable level while also allowing for multiple steady state steps. Steady state in this context refers to the state where all the solution in the tube has undergone a complete radiation cycle, in the first few steps this is evidently not the case since the solution at the end of the tube started there and has not undergone the starting parts of the tube. In steady state fresh salt solution enters the tube and fully irradiated salt solution leaves the tube with no part of receiving any less than full irradiation.

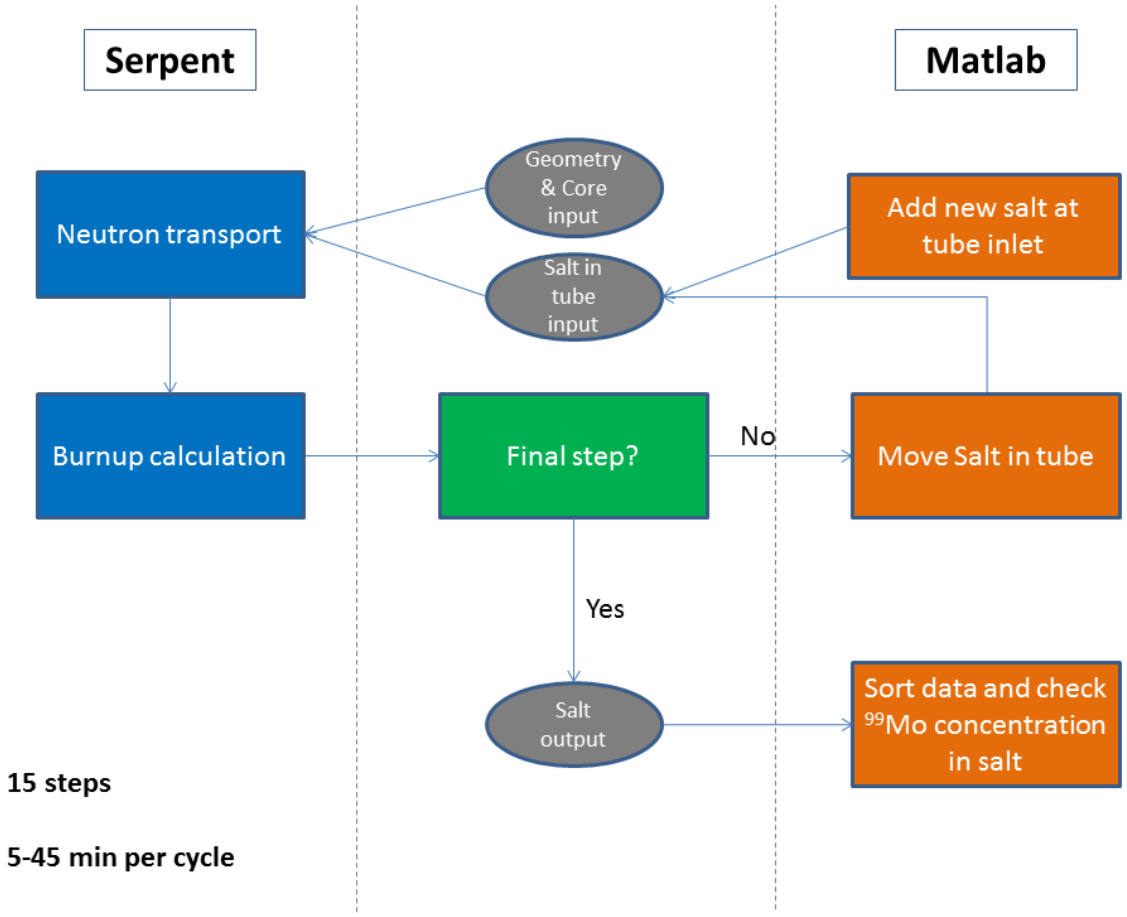

Figure 15 Schematic representation of the full simulation process

The cycle that can be seen in figure 9 is the 'neutron transport' part of the 'Serpent' section of figure 15. A cycle for the entire process starts with Serpent. Geometry, core and salt inputs are supplied to Serpent in the form of txt files. Serpent then does a burnup calculation for the salt solution. This burnup calculation gives a detailed list of isotopes inside the different sections after irradiation as an output in the form of a txt file. This txt file is then read into Matlab, where the solution in every section of the tube is moved to the next section and new, not yet irradiated salt solution is supplied at the inlet. The atomic isotope densities for all segments together with the atomic densities for the salt solution leaving the tube is then saved to a new txt file. This txt file is then read into Serpent as the new salt input and using the same geometry and core inputs a new cycle can be started. After the required number of cycles is completed, Matlab gets the ^{99}Mo concentration from the txt files that include the isotope densities at every step and these ^{99}Mo concentration are sorted and put into matrices.

Another thing to note is that Serpent detects and counts the amount of ^{235}U fissions in each segment. This is done to calculate the heat production in the salt.

2.4. Salt choice and composition

There are two uranium salts that are generally used for ^{99}Mo production in AHRs. These salts are uranyl sulphate and uranyl nitrate. Both of these salts will have uranium enrichments of 20% at maximum, as is the upper limit for lowly enriched uranium. Both salts have advantages and disadvantages as opposed to each other. These advantages and disadvantages are displayed in table 3.

Table 3 Advantages and disadvantages of the different salt types[16,17,18,20]

Uranyl nitrate	**Uranyl Sulphate**
+ Uranyl nitrate solutions are simple to prepare. One can just dissolve uranium metal plates in nitric acid.	- Uranyl sulphate solutions needs additional work to be created. The uranium metal has to either be covered in another metal or be oxidised before production is possible.
+ Uranyl nitrate has a high solubility in water (~660 g/L)	- Uranyl nitrate has a low solubility in water (~275 g/L)
+ ^{99}Mo is relatively easily recovered from uranyl nitrate	- ^{99}Mo is hard to recover from uranyl sulphate, because $(MoO_4)^{2-}$ gets more competition for sorption to in the separation column from $(SO_4)^{2-}$ and $(HSO_4)^-$ than from $(NO_3)^-$.
- In addition to H_2 and O_2, NO_x and N_2 are created, because of a low irradiation stability. These additional gasses require a bigger and more complex off-gas loop to deal with them through either extraction or recombination.	+ H_2 and O_2 are the only gasses produced during irradiation, since uranyl sulphate has a high irradiation stability. This allows for a simple off-gas loop that recombines these gasses to water.
+ No detectable amount of peroxide is formed during irradiance	- Significant amounts of peroxide are formed during irradiance. A catalyst must be added to the solution to remove this peroxide otherwise uranyl peroxide will precipitate.
- Creation of the nitrogen gasses leads to an increase in the pH of the solution. Since the pH needs to stay around 1, additional nitric acid has to be added to compensate for this gas creation.	+ The pH of uranyl sulphate remains constant during irradiation.

Weighing these advantages and disadvantages, the choice was made for uranyl nitrate. This is because the simpler off-gas system is the only major advantage sulphate has over nitrate. If one ignores the off-gas problems, uranyl nitrate is clearly superior since its superior extraction capabilities and higher solubility mean that 99Mo production using nitrate will generally have higher yields. The problems with the off-gas system means that a method for nitrate can simply be adapted to be used for sulphate by simplifying the off-gas system, therefore looking at nitrate is more useful since it supplies the higher possible isotope yield.

In order for this salt to be accurately simulated in Serpent, its atomic densities have to be known. Natural uranium generally consists of three uranium isotopes, uranium-235, uranium-238 and uranium-234. Enrichment of uranium leads to an increased mass percentage of both ^{235}U and ^{234}U. Since ^{234}U is a major α-contaminator in medical isotopes, as mentioned earlier, and since its mass percentage becomes too high to ignore for enriched uranium, the ^{234}U mass percentages needs to be known for enriched uranium. The atomic densities of the three uranium isotopes densities can be calculated if one knows the ^{235}U mass percentage and the uranium concentration in the salt solution.[18,21] Knowing these two, the mass percentage for ^{234}U can be calculated using the linearization seen in equation (2.1) with the rest of the uranium mass being made up of ^{238}U.

$$m_{pU234} = 8.44\times10^{-3}\times m_{pU235} - 7.0084\times10^{-4} \quad (2.1)$$

$$m_{pU238} = 100 - (m_{pU235} + m_{pU234}) \quad (2.2)$$

Where m_{pU234}, m_{pU235} and m_{pU238} are the mass percentages of respectively ^{234}U, ^{235}U and ^{238}U. Using these mass percentages, the particle densities of these different uranium isotopes in the solution can be calculated.

$$N_i = \frac{w_i C_U}{A_i} N_A \tag{2.3}$$

Where N_i is the atomic density of isotope i in cm^{-3}, C_U is the uranium concentration in the water in g cm^{-3}, A_i is the atomic mass of isotope i in g mol^{-1} and N_A is Avagadro's number in mol^{-1}. Once one has these atomic densities, the mass of the fuel can be determined using equation (2.4). The atomic densities of nitrogen and oxygen in uranyl nitrate can also be calculated using equation (2.5) and (2.6).

$$m_{Fuel} = \left(\frac{N_{234}B_{234}}{N_A} + \frac{N_{235}B_{235}}{N_A} + \frac{N_{238}B_{238}}{N_A}\right) \times 1000 \tag{2.4}$$

$$NN = 2(N_{234} + N_{235} + N_{238}) \tag{2.5}$$

$$NO_{UO_2(NO_3)_2} = 8(N_{234} + N_{235} + N_{238}) \tag{2.6}$$

Where m_{Fuel} is the fuel mass in g, and B_i is the atomic mass of uranyl nitrate with an atom of uranium isotope i in atomic mass units or gram per mole. The multiplication by 1000 is because all atom densities are normalised over 1 L of salt solution . The formulae for the atomic densities of nitrogen and oxygen in uranyl sulphate come from the fact that uranyl nitrate is $UO_2(NO_3)_2$, so for every uranium atom, there have to be 2 nitrogen atoms and 8 oxygen atoms. Using the fuel mass, the volume of the fuel can be calculated using the fuel's density. And the rest of this 1 L volume is then taken up by the water.

$$v_{Fuel} = \frac{m_{Fuel}}{\rho_{Fuel}} \tag{2.7}$$

$$v_{Water} = 1000 - v_{Fuel} \tag{2.8}$$

From this water volume the atom densities of hydrogen and oxygen in water can be calculated using equation (2.9) and (2.10).

$$NH = \frac{2\frac{v_{Water}\rho_{Water}}{A_{water}} Na}{1000} \tag{2.9}$$

$$NO_{H_2O} = \frac{\frac{v_{Water}\rho_{Water}}{A_{water}} Na}{1000} \tag{2.10}$$

Where v_{water}, ρ_{water} and A_{water} are respectively the volume, density and atomic mass of water. The division by thousand is once again because the atoms are spread over a volume of 1 L. The total oxygen atomic density is then given by the sum of the atomic oxygen densities given by water and uranyl nitrate.

$$NO = NO_{UO_2(NO_3)_2} + NO_{H_2O} \tag{2.11}$$

The heat capacity of the salt was determined using a linearization on reported data.[22] Heat capacities of different salt concentration were plotted and through a linear interpolation the heat

capacity for a needed salt concentration can be found. The data point and the used linear fit can be found in figure 16. The density of the salt was given in literature and is equal to 2.807 g cm^{-3}.

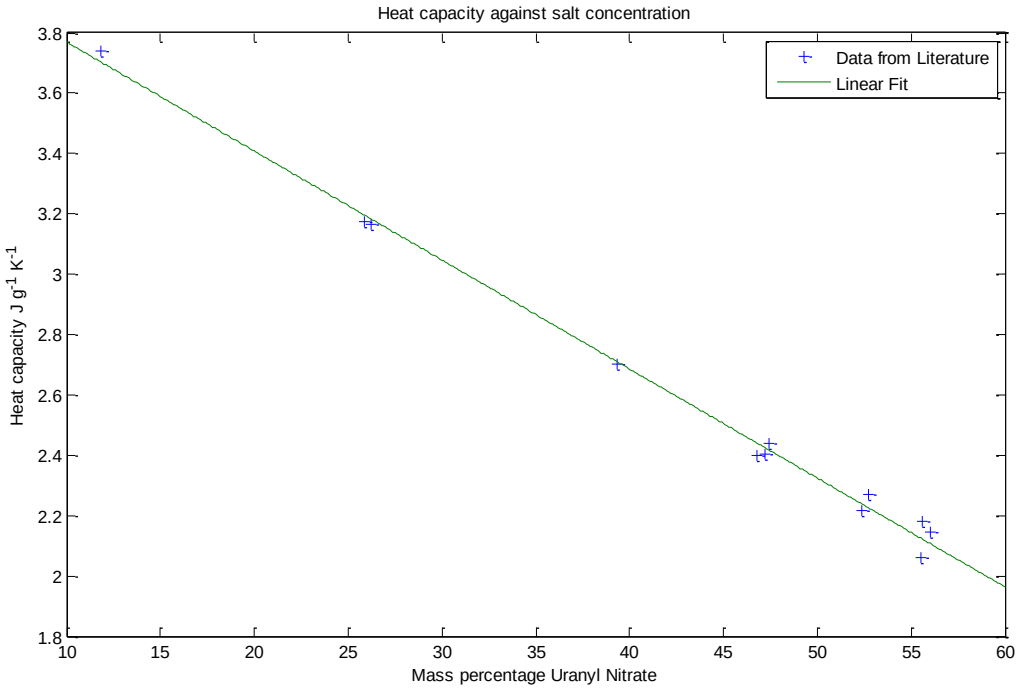

Figure 16 A linear fit for determination of the heat capacity of the salt solution at a range of salt concentrations

3. Results

All results found below use an uranium concentration of 500 g U L^{-1} unless otherwise stated. It should also be noted that when comparing two situations or setups, the same seed is used for both simulations. This is to make sure that the results of the two are comparable and that stochastic processes do not affect the results of multiple simulation in different ways, which could lead to a biased comparison.

3.1. Geometry comparison

For the initial comparison between the short, simple and accurate geometries an irradiation time of 6 days was used. This irradiation time was based on an average of irradiation times used for irradiation of LEU targets[11,23,24] since as stated in the paragraph 1.4, LEU target irradiation is the most comparable conventional isotope production technique. Having a full 6-day irradiation time means that salt stays in each segment for half a day, since as mentioned earlier this simulation consists of 12 segments. Half a day in a segment gives a total of 6 days in which the salt is in the U-tube. Figure 17 shows the concentration of ^{99}Mo in the outflow of the salt as a function of time. As expected this value increases, since in the beginning every new segment of salt that reaches the outflow has been irradiated longer than the previous one. After 6 days, this outflow concentration reaches its cap, and all following salt has a concentration around this level with some variance. The large jumps ^{99}Mo concentration in both figures can be explained by the position of salt in the tube. At every jump, salt in the tube was at one of the two places in the U-tube that was closest to the reactor core. Being this close to the reactor core leads to a significant amount of ^{235}U fission reactions and therefore to high jumps in ^{99}Mo concentrations. Figure 18 shows the medical isotope concentration as a function of its position in the tube once the simulation has reached a steady state. Steady state in this context means that enough cycles have been completed that all the salt in the tube has undergone a full irradiation cycle. In this case, it would take 6 days of irradiation before steady state is achieved. It should be noted that the concentration in both these figures is given in the unit barn^{-1} cm^{-1} which is the conventional unit used for simulations of this kind. This unit equivalent to 10^{24} cm^{-3} which in the concept of atomic densities means there are 10^{24} atoms in a cubic centimetre of salt solution.

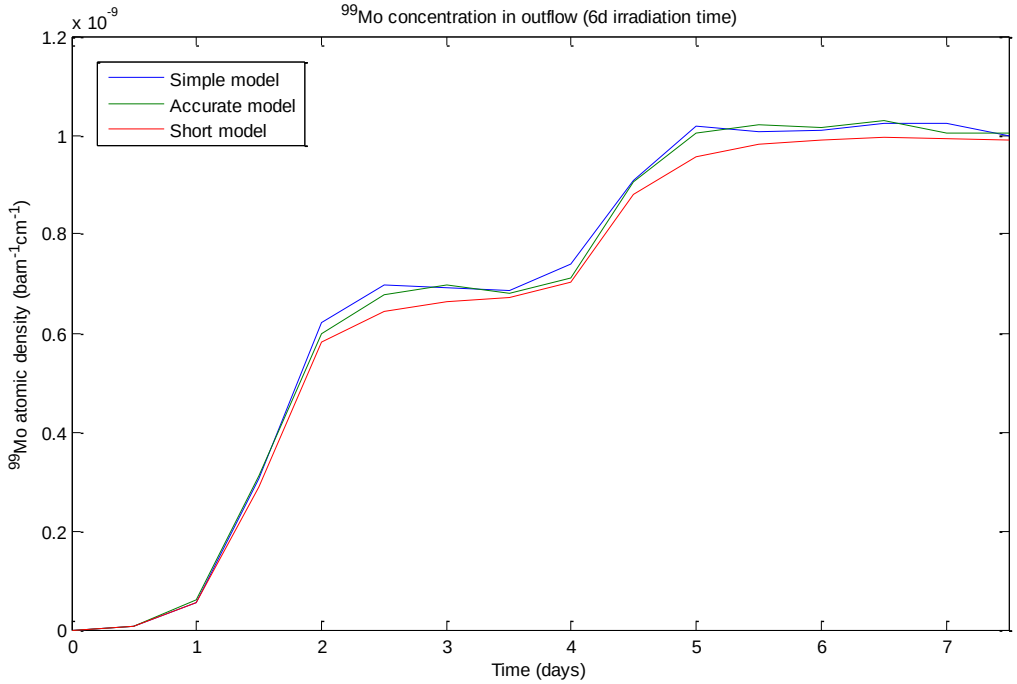

Figure 17 ^{99}Mo outflow concentration over time for an irradiation time of 6 days for a range of geometries

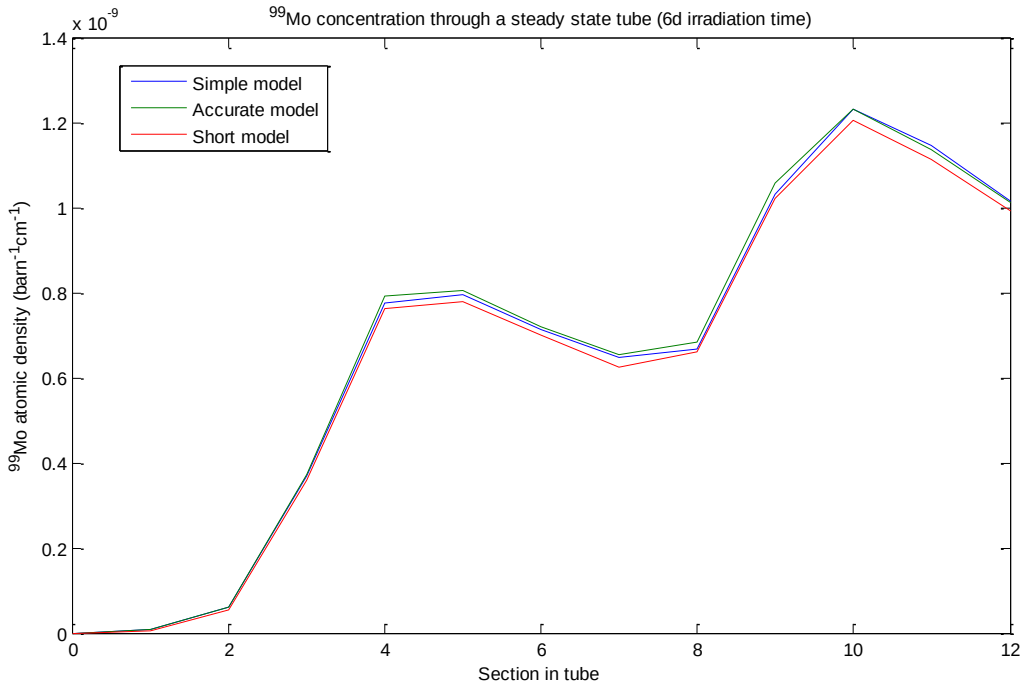

Figure 18 Steady state ^{99}Mo concentration in the U-tube for an irradiation time of 6 days for a range of geometries

Comparing the three models, one finds that the average amount of ^{99}Mo that is produced weekly is 1.85 mg for the accurate model, 1.82 mg for the short model and 1.86 mg for the simple model. This is equivalent to a weekly production of respectively 196.3, 192.5 and 196.9 6-day curie, so about 1.6% of the weekly world demand for ^{99}Mo. Comparing both simplified models to the accurate model, one sees that on average the simple model has a difference of 4.2% to the accurate model and only 2.3% if one only looks at outflow salt concentrations. For the short model this becomes 5.7% and 3.9%

Looking at figure 18, it should be apparent that the initial 6-day irradiation time has a flaw in that between some segments, the amount of new ^{99}Mo produced is smaller than the amount lost through decay. This effect is barely visible in figure 17, since this figure shows only the outflow concentration of medical isotope. So while inside the pipe concentrations can be lower between segments, at the outflow the isotope concentration increases since all the salt undergoes this effect but the longer the simulation runs, the more the salt is irradiated which leads to a higher outflow concentration. This problem could be fixed by increasing the speed at which that salt flows through the pipe, effectively lowering the irradiation time per segment. Doing this should lower the production per segment, but should also give the ^{99}Mo less time to decay and increase the total amount of segments that are produced . An irradiation time of 2 hours was chosen to see if the decay effect could be compensated by speeding up the salt flow in the tube. Although the flow speed of the salt in this case is higher than realistically would be used, the results can still show a trend of whether increasing flow speed can lead to better isotope production. Results of this 2 hours irradiation time simulation can be seen in figures 19 and 20, with 19 being the steady state situation and 20 being the outflow concentration.

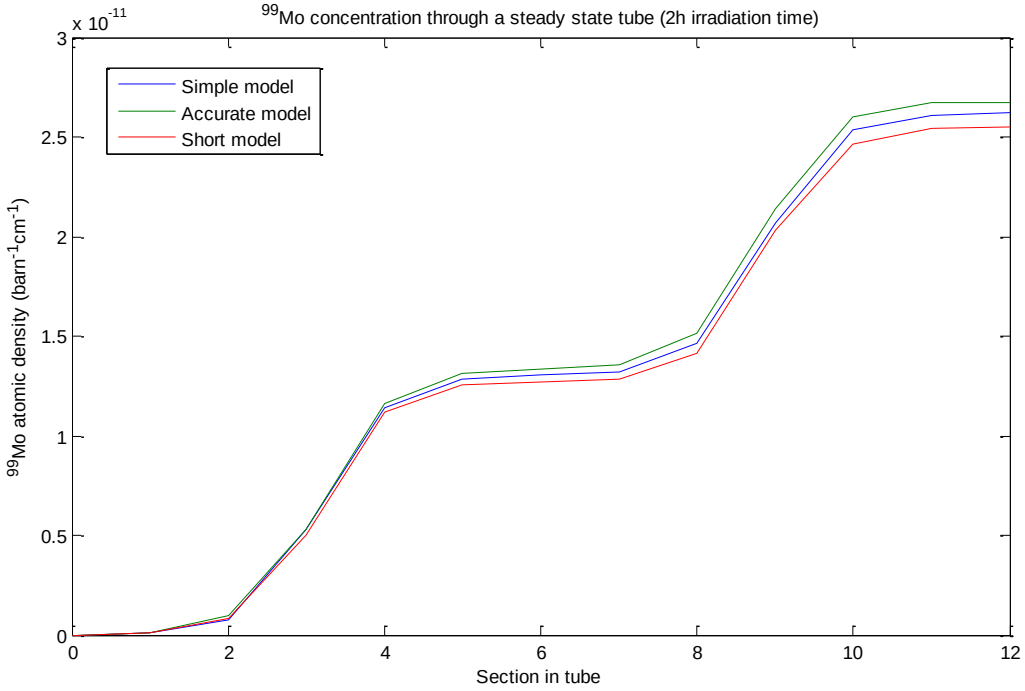

Figure 19 Steady state ^{99}Mo concentration in the U-tube for an irradiation time of 2 hours instead of 6 days

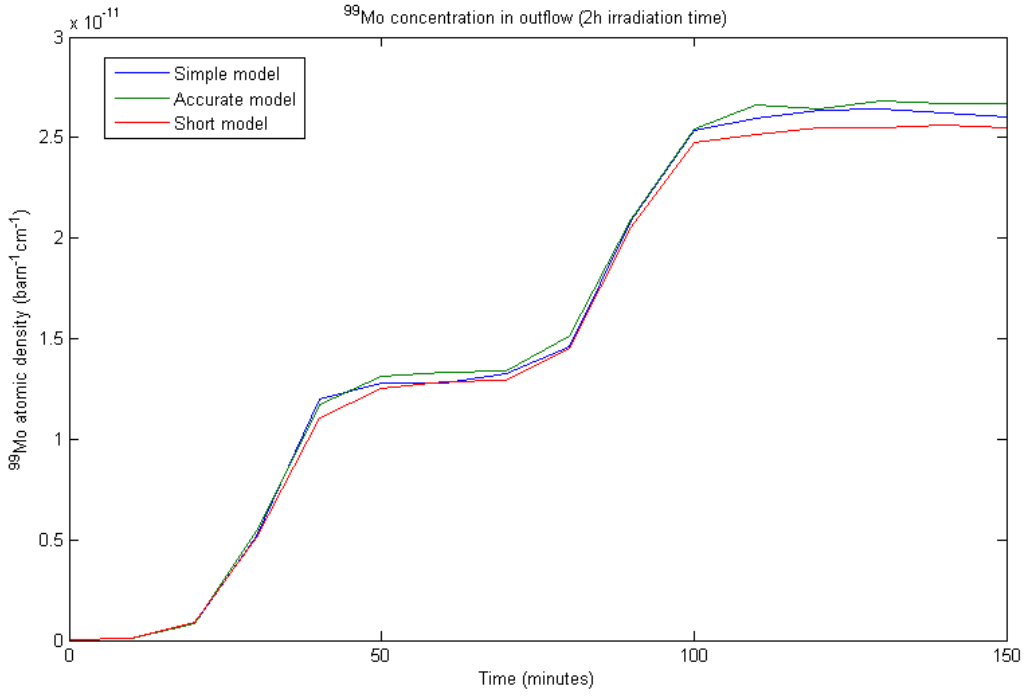

Figure 20 ^{99}Mo outflow concentration over time for an irradiation time of 2 hours instead of 6 days

Looking at figure 19, one sees that increasing the flow speed and therefore decreasing the irradiation time does in fact compensate for the decay of ^{99}Mo. No more dips in concentration can be found when looking at the steady-state. Comparing the three models for this two hour irradiation time, one finds that the average weekly ^{99}Mo production now is 3.53 mg for the accurate model, 3.36 mg for the short model and 3.46 mg for the simple model. This is equivalent to a weekly production of

respectively 373.4, 356.2 and 366.2 6-day curie, which is about 3% of the weekly worldwide demand for ^{99}Mo.
Comparing both simplified models to the accurate model now leads to the simple model having a difference of 5.1% to the accurate model and 2.4% if one only looks at outflow salt concentrations. For the short model this now is 6.6% and 6.0%.

Looking at the run times of the simulations, the accurate model has an average run time of 369 minutes, the simple model of 465 minutes and the short model of 331 minutes. While it should be said that run times are widely variable and depend on a number of uncontrollable variables, such as the amount of memory that is available for calculation at a given moment and the amount of users doing calculations at a given time, a general conclusion can be made from this data that the short simulation is in fact the fastest. Since the average speed increase found is of the same order of magnitude as the concentration difference found in the results, the short simulation was chosen as the geometry to be used for the rest of the calculations. This is because the decreased simulation run time is more useful than the undervaluation of isotope production that can be seen for the short simulation. In both the 6 day and 2 hour models the short simulation has an isotope production that is respectively 3.9% and 6.0% under the value of the accurate model, but this undervaluation of isotope production can be considered or compensated for.

3.2. Material between U-tube and outer tube

Figure 21 shows an XZ plot of the reactor geometry and specifically the area between the U-tube and the outer tube. This area will be filled with either air, vacuum or water for this investigation.

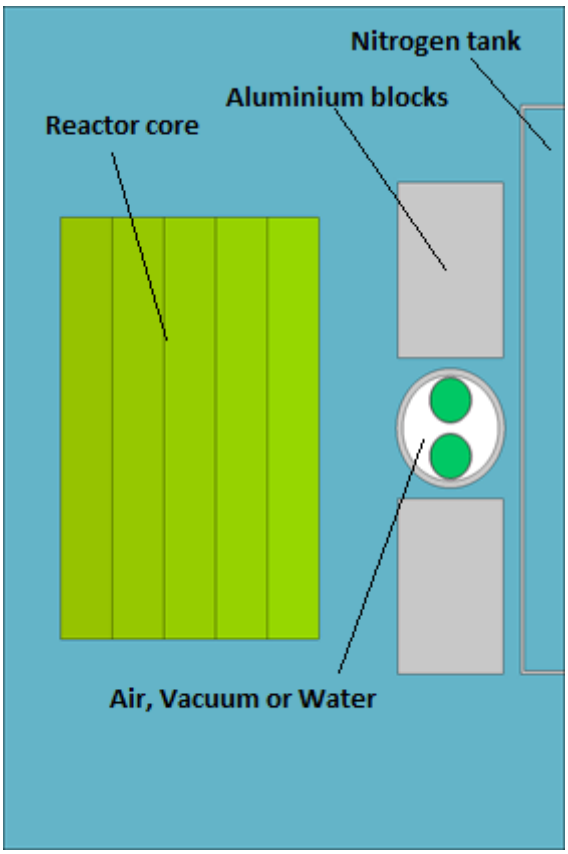

Figure 21 Space between tubes filled with air

These simulation were done to investigate whether it is beneficial for isotope production to add water in this tube, since the additional moderation could lead to additional thermal neutrons to be used in ^{235}U fission, and to see if there is a significant difference between having this area filled with air or vacuum. Making sure the area is in vacuum would require additional machinery such as a vacuum pump. If air gives a result that is equivalent to a vacuum, this sort of equipment could be kept out of the system, making the entire process simpler. Figures 22 and 23 once again show the steady state and outflow concentrations for the different simulations. It should be noted that for6-day irradiation time model is used for this simulation. This is because the 2 hour irradiation time has an unrealistically high flow speed and was mostly used to test the assumption that the concentration loss caused by isotope decay that is higher than production can be compensated by an increase in flow speed.

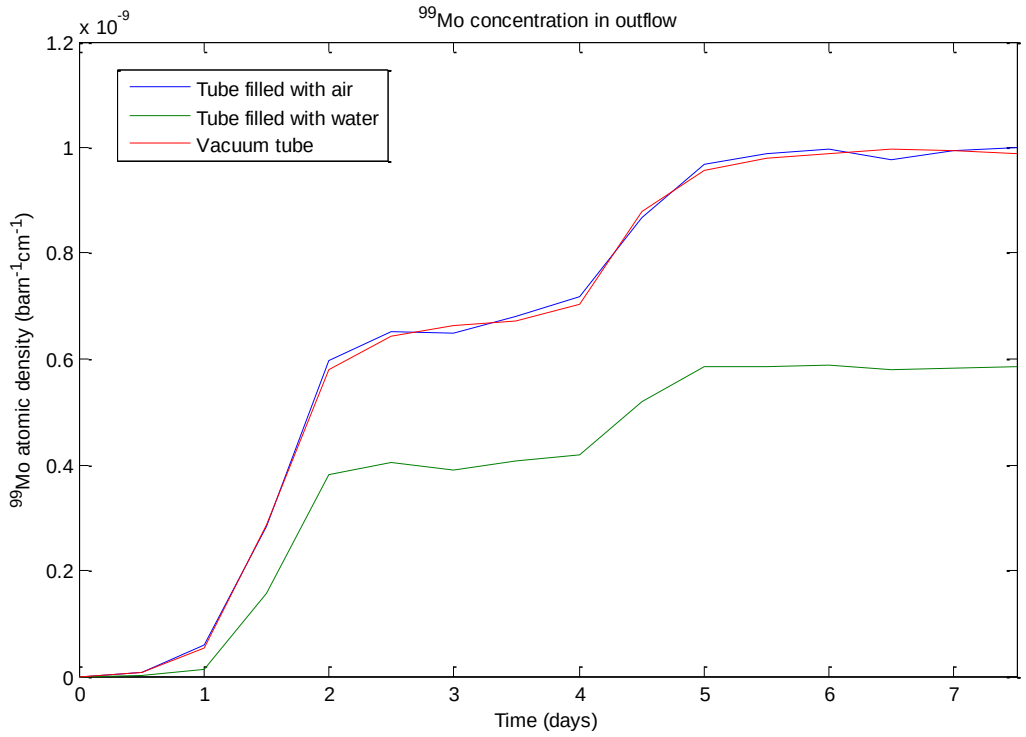

Figure 22 ^{9}Mo outflow concentration over time for different outer tube materials with a 6 day irradiation cycle

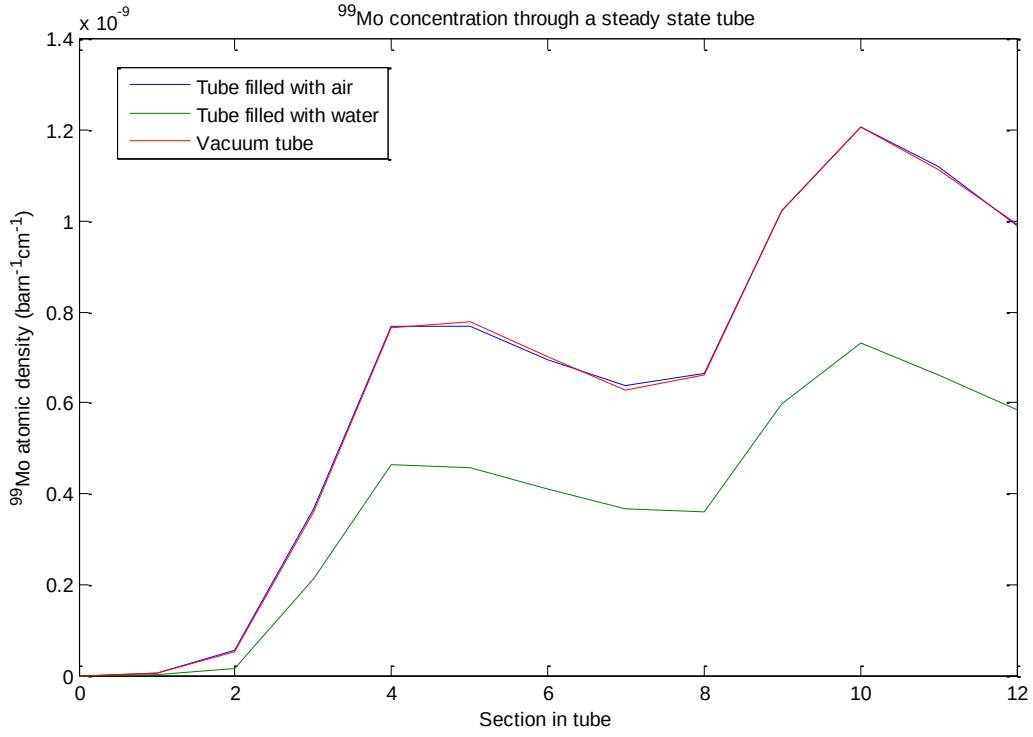

Figure 23 Steady state ^{99}Mo concentration in the U-tube for different outer tube materials with a 6 day irradiation cycle

These figures show that the increase in moderation by water is not desired because leaving the tube filled with air or in vacuum gives better results. They also show that a system filled with air and a vacuum system are all but equivalent. This means air will be used for calculations looking at the final, most feasible isotope production. The reason water does not increase neutron production is

that the additional moderation done by water is not needed. The reactor basin as it can be seen in figure 21 is more than capable of supplying an adequate amount of moderation for the neutrons coming from the core. This means that any additional moderation done by filling the outer tube with water is not needed. The amount of neutrons that is lost because of the extra interactions happening in the water is larger than the amount of thermal neutrons the water actually supplies by moderation. Therefore it is better to use a material that interacts as little as possible. Vacuum and evidently air has little to no reactions with the neutrons from the core, meaning that none are lost here and therefore meaning that more can react with the salt solution inside the U-tube. The water between the reactor core and the U-tube is used to supply moderation, but if one was able to move the U-tube closer to the reactor core, it might become more viable to add the water in the outer tube for moderation. This means that the result found here is only valid if one doesn't move the position of the outer tube in the reactor geometry.

3.3. The Orientation of the U-tube

There are several positions in which the U-tube can be oriented inside the outer tube. A comparison will be made between the most extreme situations. The first of these two extremes is the situation that has been used in the previous simulations, where the two part of the U-tube are above each other as can be seen in the third set up in figure 24 for example. This situation will be referred to as Ω-max, since the amount of angles a neutron can have while reaching the salt is maximized in this situation. The other extreme is when the two parts of the U-tube are next to each other, as can be seen in the first two set ups in figure 24. This situation will be referred to as R-max, since the distance of which a neutron can interact with the salt is maximized in this situation. This is because, looking at a neutron that comes in from the front from the side of the core, a neutron can go through the full length of the two parts of the U-tube filled with salt solution in which it can react with this solution. This is twice as much as a neutron in the Ω-max orientation which can at max go through one U-tube part length at max. There are two versions of R-max, R-max 1 and R-max 2. The difference between these two is that, looking at figure 24, in the case of R-max 1 the salt enters the U-tube through the left part. This means that the salt will have the shortest distance to the core and therefore the highest neutron irradiation at the start of its cycle, while flowing into the system. R-max 2 is the opposite situation where salt flows in from the right side and the highest irradiation is found at the end, when the salt is flowing out of the tube. Figures 25 and 26 respectively show the steady-state concentration and the outflow concentration

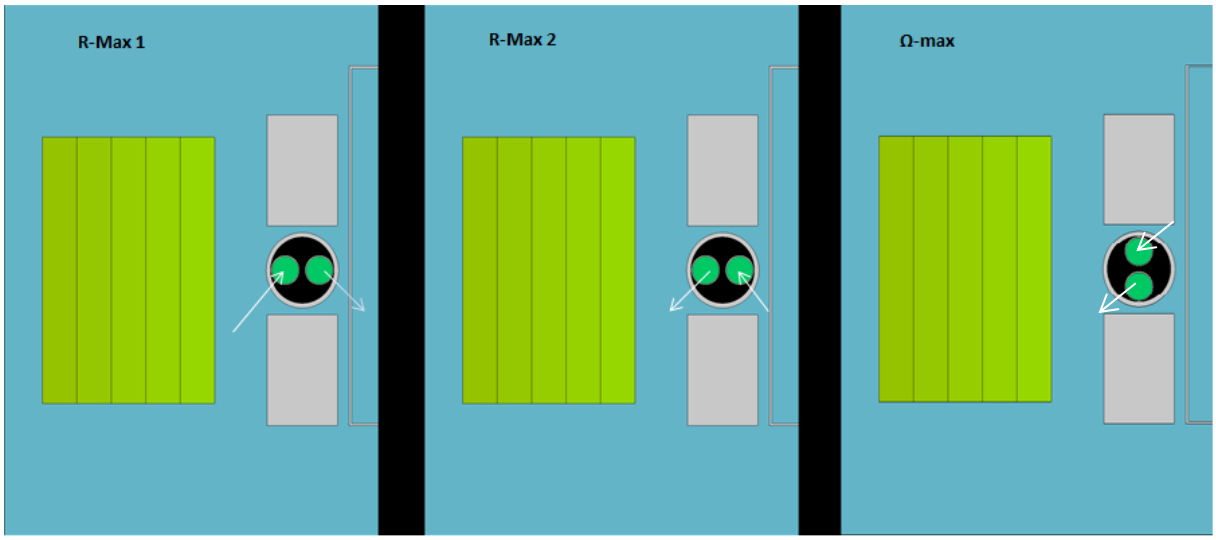

Figure 24 YZ plots of the different orientations

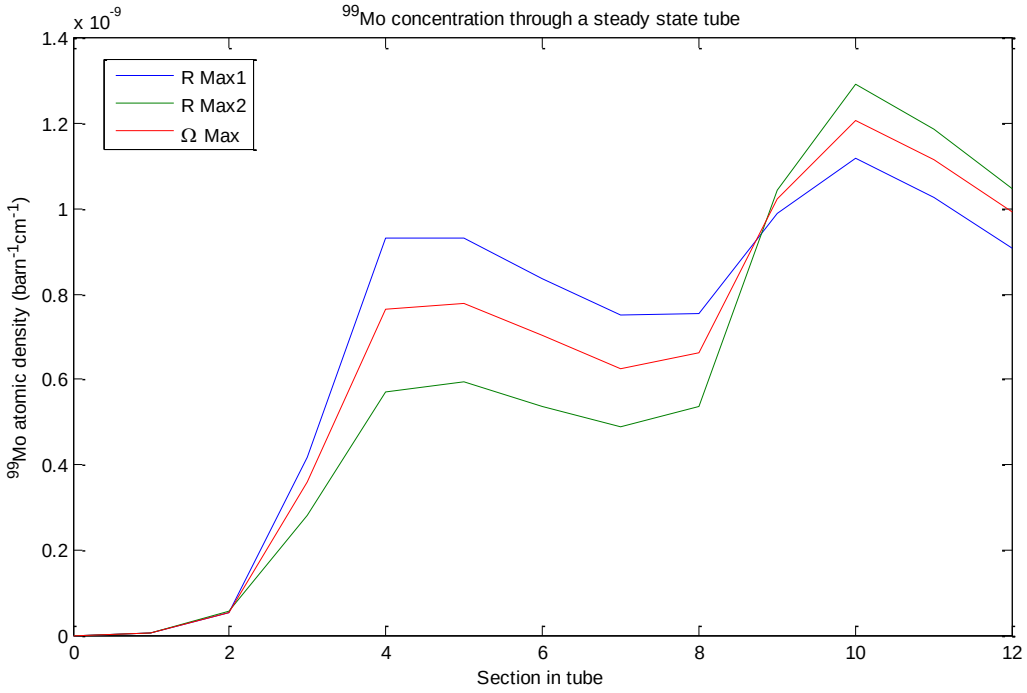

Figure 25 Steady state ^{99}Mo concentration in the U-tube (6 day irradiation time, vacuum)

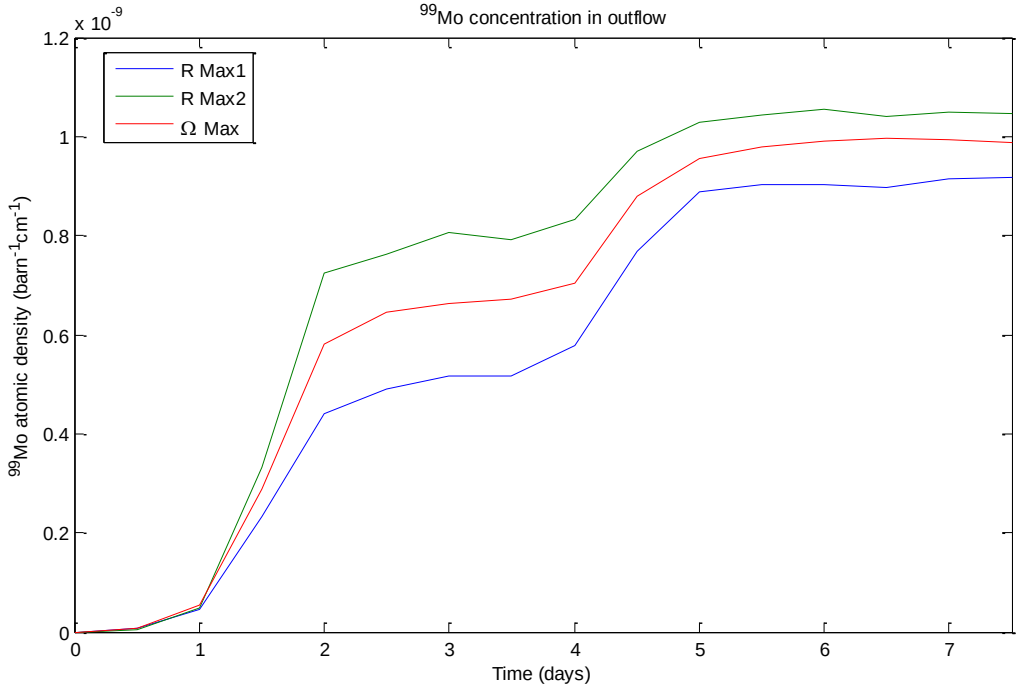

Figure 26 ^{99}Mo outflow concentration over time (6 day irradiation time, vacuum)

As can be seen in the figures , R-max 2 yields the most ^{99}Mo. This is caused by the high decay that is present during the 6-day irradiation time simulation. Since a lot of ^{99}Mo decays during a cycle through the U-tube, it is convenient to have the bulk of irradiation done as late as possible, to minimize the amount of ^{99}Mo that can be lost through decay. The more uniform high irradiation is just incapable of sufficiently compensating for decay and therefore a burst of radiation at the end of the cycle is more effective. Since the problems with the 6-day irradiation cycle are the cause of these results, the 2-hour irradiation cycle was once again used to see if the results would differ in this case.

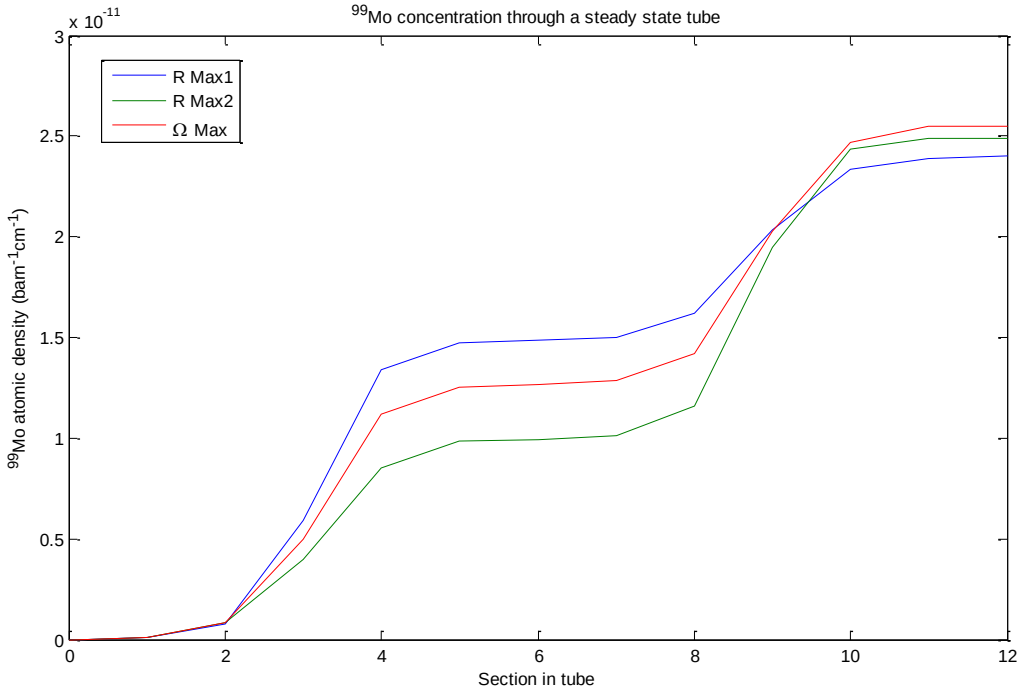

Figure 27 Steady state ^{99}Mo concentration in the U-tube (2 hour irradiation, vacuum)

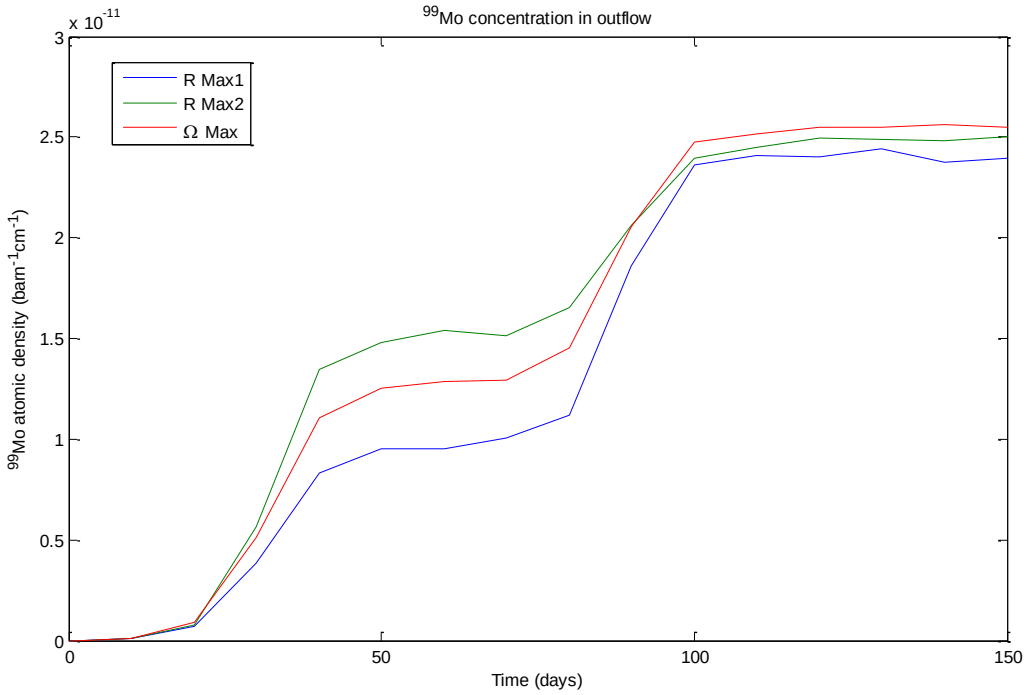

Figure 28 ^{99}Mo outflow concentration over time (2 hour irradiation, vacuum)

As can be seen in figure 27 and 28 , the more spread out irradiation intensity given by the Ω-max setup is superior given a 2-hour irradiation cycle. When decay is significantly reduced, Ω-max provides a higher isotope production. R-max 1 will give the least amount of ^{99}Mo in all cases, since high irradiation at the start of a cycle is just not worth it because of either decay, which still is a minor factor even in the higher speed cycles, or a preference for just more consistent irradiation through the loop as is the case for Ω-max. This shows that given a higher cycle speed, it becomes more and more desirable to go for a setup that produces irradiation that is as high as possible over as

long a period as possible, while lower cycle speeds lead to a preference of setups that do as much of the irradiation as late as possible.
Resulting from these simulations, either R-max 2 or Ω-max will be chosen for calculations looking at the final, most feasible isotope production depending on the irradiation time used for these calculations.

3.4. Effect of the salt concentration of the inlet flow on ^{99}Mo production

As was noted in the introduction, in AHRs increasing the concentration of the uranium salt used as fuel will not always lead to a higher yield. In the case of classic LEU and HEU targets however, more uranium in the targets does increase the isotope production. To see whether the uranium salt solution in this setup has the same uranium concentration dependence as the salt in an AHR or as classic targets, simulations were done at different salt concentrations to see the effect this concentration has on ^{99}Mo production. Figure 29 shows the results of these simulations. It can be seen that an increase in salt concentration does lead to an increase in isotope production. Once again this supports the idea that the behavior of the salt in the U-tube under irradiation is more comparable to a LEU target than to the behavior of the salt under irradiation in an AHR. The amount of isotopes produced seems to asymptotically increase with the uranium concentration in the solution, reaching this cap at around 550 to 600 g U L^{-1}. Presumably this cap is caused by the fact that there is a maximum of neutrons that could react with ^{235}U to create ^{99}Mo and a further increase in ^{235}U past this maximum can therefore not generate more ^{99}Mo. Resulting from this assessment, the maximum possible uranium concentration will be used for calculations looking at the final, most feasible isotope production. This maximum will however be bound by other factors such as the ^{99}Mo extraction capability at different salt concentrations.

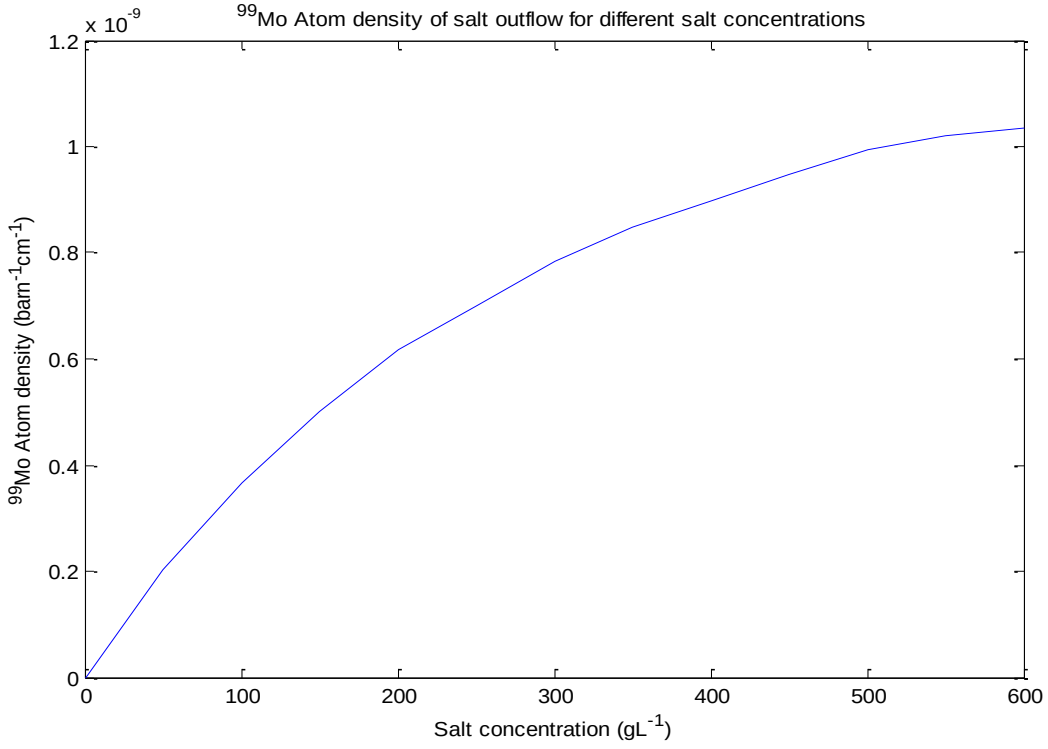

Figure 29 ^{99}Mo output concentration as a function of uranium concentration in the solution

3.5. Influence of ^{99}Mo extraction capability on potential yield

Using the results of previous simulations and applying boundary conditions on production, a simulation can be made to truly assess the viability of ^{99}Mo production using this method of uranium salt targets. Literature research shows that while classic alumina separation columns cannot effectively be used for salt with an uranium concentration higher than 150 g U L^{-1}, Thermoxid and PZC can effectively extract 99Mo from an uranium salt for concentrations up to 310 g U L^{-1}.[16] This can also be seen in figure 7. Assuming that the plant extracting the isotopes uses these alternative sorbents, this 310 g U L^{-1} concentration can be used for the simulation. Since it was found in section 3.4 that a higher uranium concentration in the salt results in a higher ^{99}Mo yield, 310 g U L^{-1} will be the concentration used in this simulation.

Literature also shows there is a time constraint to ^{99}Mo production. Salt solutions need to stay in the columns for at least 15 minutes for ^{99}Mo to be sufficiently extracted.[16] When one makes the assumption that all salt leaving the U-tube is sent directly to an extraction plant, this means that salt needs to spend at least 15 minutes in each segment. Since through comparison of the 6-day and 2-hour situation one is led to believe that a short irradiation time is optimal, this minimum of 15 minutes per segment will be used. Assuming this model were salt solution continuously flows from segment to segment, this leads to a 12 segments long U-tube where salt solution flows through the tube at a speed of 15 minutes per segment, leading to a total cycle time of 3 hours.

The amount of salt solution a facility can process is a quantity that is generally not mentioned in literature. One can assume however that since the amount of ^{99}Mo produced at this facility will be relatively small, massive extraction plants should be able to deal with any amount of liquid produced in it. Furthermore, in the case that this facility builds its own extraction plant, the amount of liquid that can be processed is mainly dependent on the size of the extraction column, since a larger column is able to extract ^{99}Mo from larger volumes of liquid. An extraction facility built at the facility itself can therefore just be made large enough no matter how much liquid the system processes.

Since the irradiation time is 3 hours, the Ω-max U-tube orientation will be used as it was seen this orientation is preferable for lower irradiation times. The area between the U-tube and the outer tube is filled with air since it is practically equivalent to vacuum, while also being more practical to use in an actual setup.

Three simulations were done under these constraints. All three of these simulations are done with the same parameters for geometry, the salt etc. but with a different, random seed for each simulation. The reason three simulations were done was to be able to take an average of these three to make sure randomness would not significantly alter the final result, since unlike in previous cases were different situations were compared using the same seed, these runs were with a random seed specifically to find how much ^{99}Mo this system would produce . Figure 30 shows the steady state concentration flow through the U-tube and figure 31 shows the ^{99}Mo concentration in the outflow. The names main 1, main 2 and main 3 refer respectively the first, second and third run of this main simulation.

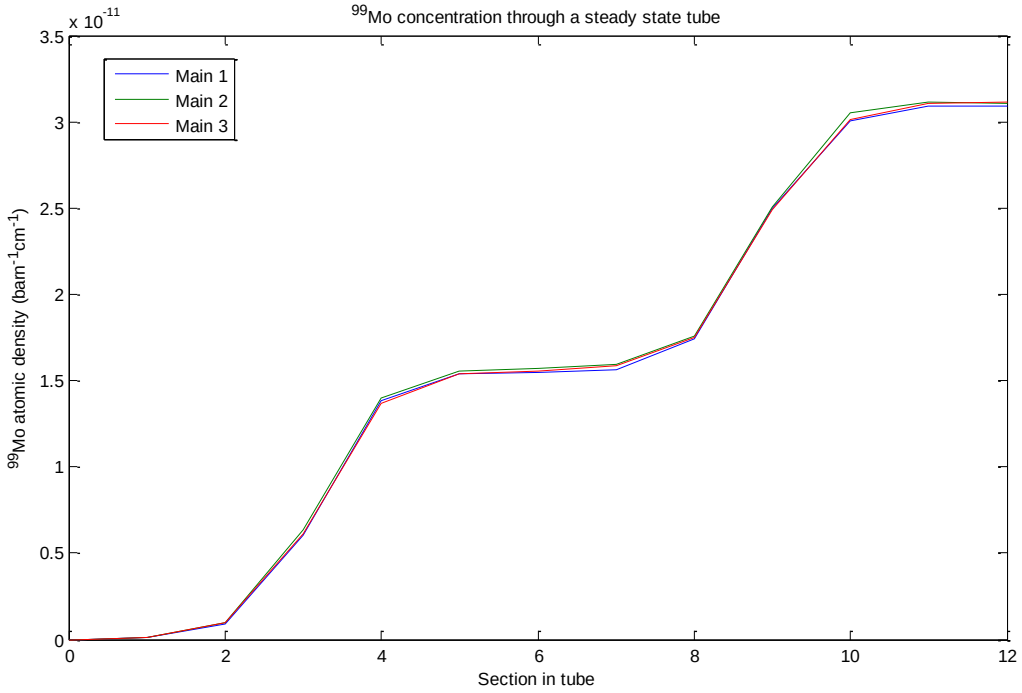

Figuur 30 Steady state ^{99}Mo concentration in the U-tube for salt under boundary conditions of extraction under 3 hour extraction time, with an air filled outer tube in the Ω-max orientation

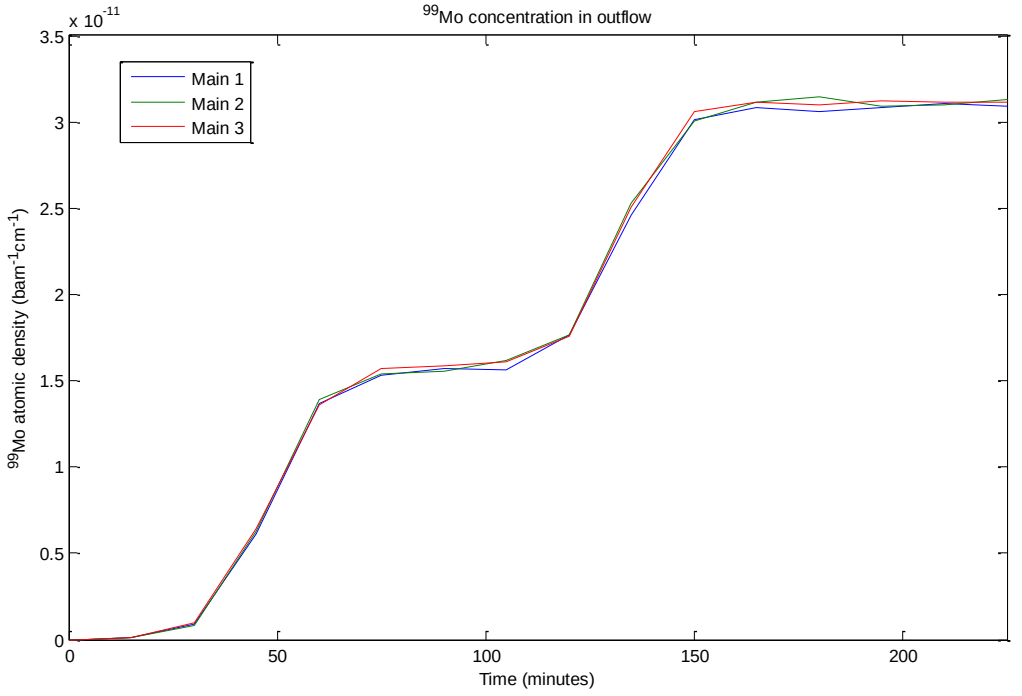

Figure 31 ^{99}Mo outflow concentration over time for salt under boundary conditions of extraction under 3 hour extraction time, with an air filled outer tube in the Ω-max orientation

On average the weekly ^{99}Mo production is 2.73 mg which is equivalent to 289 6-day Curie, which is around 2.4% of the weekly worldwide demand for ^{99}Mo.

3.6. Safety assessment

To assess the safety of the uranium salt method of 99Mo production, two extremes were tested. The two following situations were considered:

- The water leak, where a hole in the outer tube causes water from the reactor basis to leak into the outer tube and fill it completely.
- The salt leak, where a leak in the U-tube causes the area between the outer tube and the U-tube to completely fill with uranyl nitrate.

Both these leaks can be seen in figure 32.

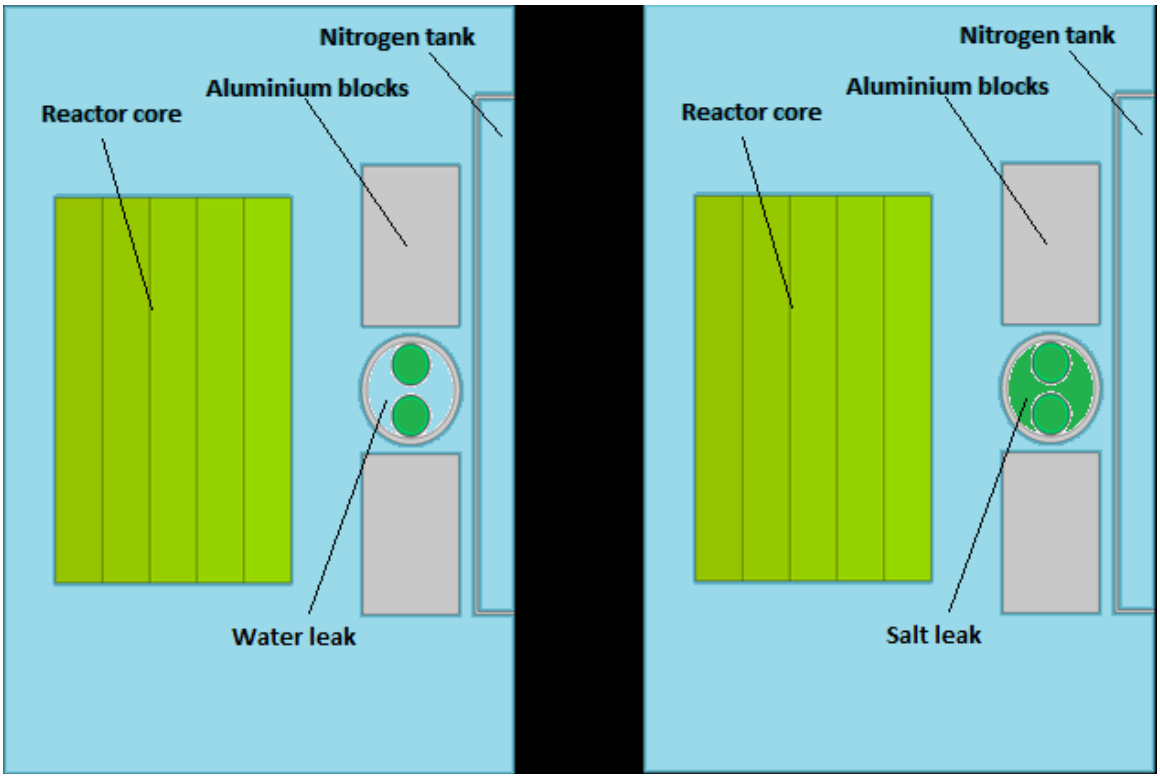

Figure 32 YZ plots of the two leak scenario's

The first assessment made of these two situations is an analysis of the k-factor, which Serpent calculates for a system by default. The core has a k-factor of 1.00904 with an uncertainty of 0.00057. In the normal case, where the core is in the reactor basin and the outer tube and U-tube are filled with air and uranyl nitrate respectively, this k-factor increases to 1.04617 with an uncertainty of 0.00058. This increase in k-factor is caused by reflections and reactions in the basin on one hand and by reactions in the U-tube on the other hand, even though it should be noted this second contribution is small. Leaking water into the outer tube leads to a change in the k-factor to 1.04453 with an uncertainty of 0.00055. Leaking salt into the outer tube changes the k-factor to 1.04622 with an uncertainty of 0.00060. The changes in the k-factor are as one would expect. The water leak lowers total 99Mo production and thus the total amount of reactions because of an excess of moderation and neutron interactions as was stated in paragraph 3.2. This lowered amount of reactions obviously leads to a lower k-factor. Following the same logic, filling the outer tube with salt solutions leads to more ^{235}U reactions and therefore a higher k-factor.

Even though a change in k-factor can be noticed because of the leaks, these changes are small and within 2 standard deviations of each other. This means that no significant change in the k-factor will be detected in case of a leak, which is generally undesirable a safety perspective because it means it will be harder to detect a leak.

The second safety assessment that was made was to check the fission power production in the tubes. To calculate this, the amount of fission reactions was measured in Serpent using detectors for the reaction rate, the volume of the segments and the time of irradiation. Assuming every reaction leads to 200 MeV of heat, all of which is absorbed inside the water, and knowing the amount of reactions that take place, the heating in the tube can be simulated if one also has the heat capacity of the salt, which was given in paragraph 2.4. Equation (3.1) shows how the temperature increase was calculated:

$$\Delta T = \frac{N_R \times 200\,MeV}{m_s C_s} \tag{3.1}$$

Here ΔT is the temperature difference in K, N_R is the number of reactions calculated by the detector in the simulation, m_s is the mass of the salt in kg and C_s is the specific heat capacity of the salt in J kg^{-1} K^{-1}.
It was found that in the normal situation, the salt heats up 37 K between entry into the U-tube and exit. When water leaks into the outer tube, this is lowered to 23 K because of the lowered total reaction rate as mentioned earlier, furthermore the added water would further lower the temperature gain inside the tube because of heat absorption by the leaked water. Lastly it was found that when salt enters the outer tube, the temperature increase in the U-tube itself will lower to only 29 K, but the salt in the outer tube will quickly heat up, causing the water in the solution to boil. Figure 33 shows a plot of the temperature increase in all three cases through sections in the tube.

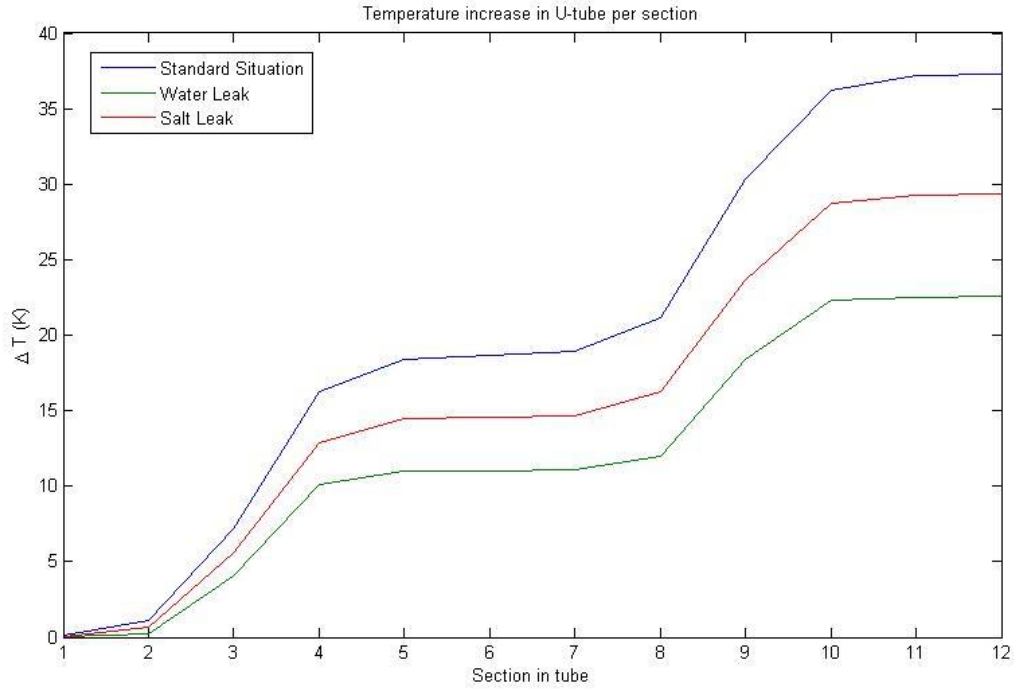

Figure 33 Temperature increases as a function of position inside the tube for the 3 hour irradiation time system with and without a leak

The temperature of the salt is therefore a good way of safety assessment, a decrease in the outflow temperature of the salt could be a clear indicator of a leak, furthermore in the case of a salt leak, the boiling of the leaked salt should be quickly found. This means that a worst case scenario as pictured here where the entire outer tube is filled with salt should never be able to happen.

4. Conclusion

Conclusively, the first thing that can be said is that the short geometry is in fact sufficient for simulations of the RID reactor core. The short model is about 10% faster than accurate model which was found to be the second fastest model, while only having a difference in isotope production of 6% compared to the accurate model. This means simulations which needs less computational power can be done, leading to more simulations in a given timespan. It should be noted that the simplified model had run times that were unexpectedly significantly higher than that of the more accurate model. This could be caused by cluster problems or by the simple model simulations having a lower priority on the cluster by random chance. It could therefore be useful to further test the simple simulation to see if lower run times are possible.

On filling the space between the U-tube and the outer tube, it can be concluded that having as little obstructive material, such as water, as possible is best if one wants to maximise ^{99}Mo production. The water of the reactor basin is already sufficient in moderating the neutrons released from the core and any additional water just stops these neutrons, instead of increasing the amount of possible useful, thermal neutrons. No significant difference was found between filling this space with air or keeping it vacuum. Both gave the same ^{99}Mo yield, which should not be surprising since air has little to no reaction it can undergo with the neutrons from the reactor core. Though it should be said that adding water in this area might be worthwhile if one wants to cool the U-tube, it can be concluded that from a ^{99}Mo yield perspective having air or a vacuum fill the space between the U-tube and the outer tube is optimal.

When looking at the orientation of the U-tube, conclusions are dependent on the time the uranyl nitrate spends in the U-tube. Longer irradiation times favour setups where the U-tube is positioned so that part of the tube is as close to the core as possible, with this section close to the core being irradiated near the end of the irradiation cycle. Shorter irradiation times on the other hand lead to a preference of a setup where the salt is irradiated more evenly during its stay in the tube. The reason for this divide between long and short is that as time spent in the tube increase, the amount of decay that happens within the salt also increases. Because of this decay one wants to do the majority of radiation as late into the cycle as possible, to minimise loss through decay. In shorter cycles decay is less of a problem and therefore more evenly distributed irradiation leads to a higher production of ^{99}Mo overall.

On the subject of salt concentration it was found that an increase in the amount of uranium in the salt solution always leads to an increase in produced ^{99}Mo, contrary to the situation for salt in an AHR. The reason for this is that, as mentioned earlier, the reactor basin is already sufficient in moderation of core neutrons, meaning that all that's left for the salt is to have as big of a cross section for neutron capture as possible. More uranium leads to more possible target nuclides and therefore for a higher isotope yield.

Taking into account these findings and applying the boundary conditions laid upon the ^{99}Mo creation process by the capabilities of ^{99}Mo extraction facilities, namely that the uranium concentration in the salt can be no more than 310 g L^{-1} and that an extraction time of at least 15 minutes is needed, the potential ^{99}Mo production in this plant has been assessed. Under the 3 hour irradiation time and using this 310 g U L^{-1} salt solution, a weekly ^{99}Mo production of 2.73 mg, or 289 6-day Curie, was found. This is around 2.4% of the weekly worldwide demand for ^{99}Mo.

Looking at the safety of this system, one can conclude that leaking of salt or water has little to no effect on the k-factor of the system. In the normal case the k-factor is 1.04617 with an uncertainty of 0.00058. Leaking water into the outer tube leads to a change in the k-factor to 1.04453 with an uncertainty of 0.00055. Leaking salt into the outer tube changes the k-factor to 1.04622 with an

uncertainty of 0.00060. While a small change in k-factor can certainly be seen, this change is always within 2 standard errors of the normal case, meaning it is too small to lead to any sort of definitive conclusion.

Looking at the heating of the U-tube during irradiation it was found that in the normal case, the salt heats up 37 degrees during a cycle. When water leaks into the outer tube, this is lowered to 23 degrees. In the case of a salt leak it was found that the temperature increase in the U-tube itself will lower to only 29 degrees, but the salt in the outer tube will quickly heat up, causing the water in the solution to boil. This means that in the case of both a salt and a water leak, the leak will be noticeable because of a change of temperature in the liquid outflow. Furthermore, the boiling salt solution in the outer tube should also be quickly noticeable.

As a suggestion for further research, a more accurate temperature profile of the system could be made. The temperature profile in this thesis is based purely on the amount of ^{235}U fissions in a given section. While this gives a general idea of heating, it can be far more accurate and since heating is an important part of a reactor like this, it is something that should be expanded upon. Secondly, an assessment could be made using a lower uranium concentration in the salt. The 310 g U L^{-1} that was used in this thesis is only valid if Thermoxid or PZC is used for ^{99}Mo extraction. While this is possible, it will probably only happen if the RID does the extraction itself since major extraction facilities use alumina sorbents since these are fine for the standard LEU and HEU targets. A case can therefore be made to do a simulation using boundary conditions for alumina sorbents. This would lower the maximum uranium concentration to no more than 150 g U L^{-1} and it could also change the total irradiation time, since the 15 minutes per section used in this report is mainly valid for Thermoxid and PZC.

Lastly, an assessment could be done using a larger total geometry, using the accurate geometry described in the thesis but with added aluminum tubes on the sides of the core and with more of the reactor bath behind the core. By doing this irradiation time would surely increase but on the other hand, a more accurate result could be acquired. It is unknown how large the difference is between this enlarged accurate geometry and the short one used in this thesis but it could be significant. Finding out how significant could be an important addition to the simulation.

5. References

1. Image courtesy of http://www.atomicarchive.com/Fission/Fission2.shtml
2. H. van Dam; T.H.J.J. van der Hagen; J.E. Hoogenboom, Nuclear Reactor Physics, April 2005
3. L.M. Caspers; D.J. v.d. Hoek; Kernreactorkunde een beknopte inleiding fourth edition, 1979
4. Hoger Onderwijs Reactor (HOR) , 2014 http://www.tnw.tudelft.nl/en/cooperation/facilities/reactor-instituut-delft/research/facilities/hoger-onderwijs-reactor-hor/
5. Image courtesy of http://www.mallinckrodt.com/Nuclear_Imaging/Global_Mo-99_Supply_Chain.aspx
6. OECD, The Supply of Medical Radioisotopes An Economic Study of the Molybdenum-99 Supply Chain, 2010
7. OEDC, The Supply of Medical Radioisotopes: Review of Potential Molybdenum-99/Technetium-99m Production Technologies, 2010
8. Kirk Bertsche, Accelerator production options for ^{99}Mo, SLAC-PUB-14132
9. IAEA, Production and Supply of Molybdenum-99, 2010
10. Association of Imaging Producers & Equipment Suppliers, report on Molybdenum-99 production for nuclear medicine – 2010 – 2020, November 2008
11. J. L. Snelgrove, G. L. Hofman, T. C. Wiencek, C. T. Wu, G. F. Vandegrift, S. Aase, B. A. Buchholz, D. J. Dong, R. A. Leonard, B. Srinivasan, D. Wu, A. Suripto , Z. Aliluddin, Development and processing of leu targetsfor mo-99 production--overview of the anl program, 1995
12. George F. Vandegrift, Facts and Myths Concerning "MO Production with HEU and LEU Targets
13. A. Mushtaq, Disposition of plutonium-239 via production of fission molybdenum-99, 2011
14. Ulli Köster, Present day production of ^{99}Mo and alternatives, 2011
15. Image courtesy of http://nl.wikipedia.org/wiki/Molybdaat#mediaviewer/File:Molybdate.png
16. D.C. Stepinski, A.V. Gelis, P. Gentner, A.J. Bakel, G.v. Vandegrift, Evaluation of radsorb, isosorb (thermoxid) and pzc as potential sorbents for separation of ^{99}mo from a homogeneous-reactor fuel solution
17. Amanda J. Youker, Sergey D. Chemerisov, Michael Kalensky, Peter Tkac, Delbert L. Bowers, and George F. Vandegrift, “A Solution-Based Approach for Mo-99 Production: Considerations for Nitrate versus Sulfate Media,” Science and Technology of Nuclear Installations, vol. 2013, Article ID 402570, 10 pages, 2013. doi:10.1155/2013/402570
18. M.V. Huisman, Medical isotope production reactor, 2013
19. Leppänen, Jaakko. Development of a New Monte Carlo Reactor Physics Code [Uuden Monte Carlo -reaktorifysiikkakoodin kehittäminen]. Espoo 2007. VTT Publications 640. 228 p. + app. 8 p.
20. Non-HEU production technologies for molybdenum-99 and technetium-99m. — Vienna : International Atomic Energy Agency, 2013.p. ; 29 cm. — (IAEA nuclear energy series, ISSN 1995–7807 ; no. NF-T-5.4) STI/PUB/1589
21. Tegas Sutondo, Analytical method of atomic density determination of the uranyl nitrate solution system. A Calculation Note, Part of Neutronic Design Analysis of SAMOP System
22. The reactor handbook volume 2 Engineering declassified edition, may 1956
23. IAEA, Conversion Planning for Mo-99 Production Facilities from HEU to LEU, August 2010

24. Budi Briyatmoko, Boybul, Sriyono, A.H. Gunawan, H. Lubis, A. Mutalib, Abidin, Hambali, Experiences of heu to leu mo-99 production conversion
25. Aluminium Alloys - Aluminium 5754 Properties, Fabrication and Applications, Supplier Data by Aalco via Azom.com

Appendix

A. Serpent

The k-eigenvalue Criticality Source Method

A neutron chain reaction inside a reactor, such as the ^{235}U chain reaction mentioned in paragraph 1.1, is simulated with the k-eigenvalue criticality source method. The criticality source method is a Monte Carlo simulation method that proceeds in cycles (or generations) of individual neutrons. A cycle consists of a specific number of neutron histories, all taken from the same source distribution. The neutron source distribution for the first cycle has to be supplied to the program, while every source distribution after this initial entry is generated by the program itself. This is because for every cycle after the first one, the source distribution is determined by the neutron histories of the previous cycle. Once a neutron has a fission interaction, its history is terminated and the place of its reaction is added as a source point for the next cycle, meaning that the source distribution in the following cycle is equal to the resulting fission distribution in the current one. Since the initial, user defined, distribution can be far from the final distribution, a number of cycles are run but afterwards discarded at the start of the simulation. By doing this, it is guaranteed that a converged source distribution is used for all cycles of the simulation. A problem with this method is that the source size is generally different for every cycle. This can happen either systematically, when looking at a super- or subcritical system, or randomly, because of deviation in a critical system. This would lead to problems within the simulation since all calculations done by the program are done for a stationary system, where k=1. To compensate for this effect the k-eigenvalue method is used. The k-eigenvalue criticality source method is a variant within criticality source simulation that simulates a stationary self-sustaining chain reaction. This is done by adjusting the source size of a cycle to always be a specific value. In essence, neutrons are randomly added to the source distribution if k<1 and removed if k>1.

Neutron movement

To sample the movement of neutrons, the free path length between collisions is determined. To explain the concept of the free path length, it is best to think of a neutron moving through a homogenous material with a single macroscopic total cross section. The probability that a neutron will undergo an interaction moving a distance dx through this material is given by equation (A.1).

$$dP = \Sigma_t dx \tag{A.1}$$

Where Σ_t is the macroscopic cross section of the medium. When one assumes that the neutron is a distance x removed from an arbitrary zero point, $P_0(x)$ can be defined as the chance that the neutron moved a distance x through the material without any interaction. When the neutron then moves another distance dx from position x, the change in $P_0(x)$ is given by equation (A.2).

$$dP_0(x) = -P_0(x)dP = -P_0(x)\Sigma_t dx \tag{A.2}$$

Which is a differential equation that when solved gives the non-interaction probability:

$$P_0(x) = e^{-x\Sigma_t} \tag{A.3}$$

From this, the probabilty density function and the cumulative distribution function can be found as can be seen below.

$$P_0(x)dP = \Sigma_t e^{-x\Sigma_t} dx \tag{A.4}$$

$$f(x) = \Sigma_t e^{-x\Sigma_t} \tag{A.5}$$

$$F(x) = \int_0^x \Sigma_t e^{-x\Sigma_t} dx' = 1 - e^{-x\Sigma_t} \tag{A.6}$$

And from this cumulative distribution function, an equation for the free path length between two interactions, x, can be found using the inversion method. This is because the cumulative distribution function $F(x)$ is uniformly distributed and can therefore by simulated by setting an uniform random variable ξ to be equal to $F(x)$ and because these two are equal, the inversion method can be used.

The inversion method is a technique in statistics used to sample a random variable x from distribution $f(x)$. If one takes the cumulative distribution function $F(x)$, such as the one in (A.6), of this distribution, one can make an uniformly distributed variable ξ and set it to be equal to $F(x)$ over the unit interval. The value of the variable x itself can now be calculated by applying the inverse of the CDF on the uniform random variable as follows:

$$F(x) = \xi \Leftrightarrow x = F^{-1}(\xi) \tag{A.7}$$

Applying this principle to the CDF for $F(x)$ in (A.6) and therefore for the free path length x, the following equation is found.

$$F(x) = 1 - e^{-x\Sigma_t} = \xi \Leftrightarrow x = -\frac{1}{\Sigma_t}\ln(1-\xi) = -\frac{1}{\Sigma_t}\ln(\xi) \tag{A.8}$$

Where ξ is a uniformly distributed variable . The last step can be made because of this, since an useful aspect of uniformly distributed variables is that ξ and $1-\xi$ are equally distributed. Using equation (A.8) Serpent is able to simulate neutron tracks.[19]

Neutron interactions

Once a neutron reaches the site of an interaction within a material, multiple kinds of interactions are possible. Which isotope within the material is chosen to react is sampled based on the macroscopic cross sections of all isotopes inside the material. For any given material, the chance for a specific isotope to react is equal to the macroscopic cross section of this isotope divided by the total macroscopic cross section of all isotopes inside the material. This same process is used to decide which kind of reaction happens. The chance of a specific reaction is given by the macroscopic cross section for this reaction, divided by the total macroscopic cross section for all reactions of a given isotope. The three main interactions are capture, fission and scattering. If none of these interactions occur, the neutron reaches the boundary of the geometry and boundary effects occur. Depending on the boundary conditions, the neutron history will either be terminated or continued with different parameters. The choices for boundary conditions in Serpent are black, where all the neutrons reaching the boundary are treated as if they leak out of the system and are lost, reflective, where the neutrons are reflected back into the geometry, and periodic, where a neutron reaching the boundary is placed at the opposite side of the geometry.

Scattering

For Monte Carlo calculations scattering is the most complicated kind of interaction. The reason for this is that when scattering occurs the neutron history does not end, as it would for fission or capture interactions. Instead a new energy and direction have to be sampled. Both inelastic and elastic scattering can be simulated, with the resulting rules for conversation of energy and momentum applying to the two-body system of nucleus and neutron. The thermal motion of the target nucleus is generally taken into account using the free-gas model. However, this model introduces significant errors into the results if used for moderators in thermal systems such as hydrogen and deuterium in water and carbon in graphite. Therefore, Serpent can use thermal scattering cross sections for these moderators instead of their normal free-gas model cross sections.

Capture

In the context of Serpent, capture refers to any neutron-nucleus reaction that does not lead to the creation of new neutrons. Since only neutrons are being considered, even reactions that are generally not referred to as capture reactions, such as fission reactions which yield an α-particle, are seen as capture reaction since they contribute nothing to the source distribution of the next cycle. Capture interactions simply end a neutron history.

Fission

Fission in the context of Serpent refers exclusively to any fission reaction that results in one or more neutrons. The way fission is simulated in Serpent is that when fission occurs, the average amount of neutrons emitted per fission, $\bar{\nu}$, is truncated to an integer value N. At least N neutrons are then added to the source distribution, with the chance of an additional neutron being added being determined based on comparing the remaining decimal fraction to a randomly generated number ξ. This leads to the following general rule for new reaction induced source neutrons in the next cycle.

$$number\ of\ neutrons\ emitted = \begin{matrix} N+1 & if\ \ \xi < \bar{\nu} - N \\ N & if\ \ \xi > \bar{\nu} - N \end{matrix} \qquad (A.9)$$

Both prompt and delayed neutrons can be emitted, with the chance of creating a delayed neutron simply being the $\bar{\nu}$ of delayed neutrons divided by the total nubar. The time of emission for delayed neutrons is exponentially distributed and, like the neutron free path length, it can be sampled from random variables using equation (A.10).[19]

$$t = -\frac{1}{\lambda_j}\ln(\xi) \qquad (A.10)$$

Where λ_j is the decay constant of the corresponding delayed neutron precursor group and ξ is an uniformly distributed variable. The energy of each new fission neutron is sampled independently from the other neutrons. Prompt and delayed neutrons are sampled from different distributions. The total process of the k-eigenvalue criticality source method transport cycle was already shown in figure 8 in paragraph 2.1. At the start of a neutron history a neutron is given an energy, which is randomly sampled from a table of possible energies dependant on the source isotope the neutron comes from, and a direction to move in. The free path length in this direction is sampled and the neutron is moved to its collision site. At the site, the specific reaction is sampled and depending on the sort of reaction, the neutron history is ended or the neutron is sent in a new direction with a new energy. This process of creating neutron histories is repeated until the required number of neutrons

in a specific cycle is reached, after which point all the fission scores and the neutrons that come from these fission reactions are used as the source distribution for the next cycle.[19]

Burnup calculation

In addition to the standard neutron transport calculations, Serpent also supports fuel burnup calculations, which are calculations that track the depletion of a given fission fuel. The isotope balance in a fuel that is irradiated by neutrons is described by a set of Bateman equations. Equation (A.11) gives an example of a Bateman equation for an arbitrary isotope j.

$$\frac{dN_j}{dt} = \sum_{i \neq j} \left[(\gamma_{i \to j} \sigma_{f,i} \Phi + \lambda_{i \to j} + \sigma_{i \to j} \Phi) N_i \right] - (\lambda_j + \sigma_j \Phi) N_j \qquad (A.11)$$

Where N_j is the atomic density of isotope j, $\gamma_{i \to j}$ is the fractional fission product yield of j in the fission of isotope i, $\sigma_{f,i}$ is the microscopic fission cross section of isotope i, Φ is the neutron flux in the material region, $\lambda_{i \to j}$ is the decay constant of isotope i to j decay, $\sigma_{i \to j}$ is the microscopic transmutation cross section of the isotope i to j reaction, N_i is the atomic density of isotope i, λ_j is the decay constant of isotope j and σ_j is the microscopic transmutation cross section of the isotope j. The terms before the minus sign are terms of isotope production and the ones after the minus sign are depletion terms. The production terms are respectively the fission, decay and transmutation terms leading to isotope j,summed over all other isotopes. The depletion term has respectively the decay and neutron induced transmutation of isotope j to other isotopes. All the Bateman equations of the isotopes inside a material are linked by their decay and production terms. This system of linked atomic densities can then be solved as a set of first order scalar differential equation. In order for Serpent to be able to do these calculations, it needs the homogeneous fission and transmutation cross sections which it produces during transport calculation. These cross sections combined with decay constants and fission yield data libraries allows Serpent to solve the Bateman equations, which allows Serpent to output depleted fuel material compositions. Burnup calculations are done in discrete time steps. In each time step, the material cross sections are constant. After the time step, a new neutron transport cycle is done using the updated material composition. This new cycle then provides new cross sections for the Bateman equation and with these new cross sections, a burnup calculation is done.[19]

B. Aluminium tube specifics

All aluminium tubes in this rector simulation are made up of aluminium alloy 574. The specifications of this alloy can be found in the table below.

Table 4 Specifics of aluminium alloy used in simulation[25]

Element	Mass percentage presenent
Si	0.4
Fe	0.4
Mn	0.5
Mg	3.2
Al	95.5

C. Core specifics

The tables below list the atomic densities of all 20 blocks used for the simulation of the reactor core. It should be noted that in addition to these isotopes 2400 cm^3 water and 1000 cm^3 aluminium are also added to each individual block to simulate the moderator and cladding respectively. These volumes are equivalent to atom densities of respectively 0.02143 $barn^{-1}$ cm^{-1} and 0.01608 $barn^{-1}$ cm^{-1}.

Table 5 Specifics for core block 1 until 9

Isotope number	block 1 density in $barn^{-1}$ cm^{-1}	block 2 density in $barn^{-1}$ cm^{-1}	block 3 density in $barn^{-1}$ cm^{-1}	block 4 density in $barn^{-1}$ cm^{-1}	block 5 density in $barn^{-1}$ cm^{-1}	block 6 density in $barn^{-1}$ cm^{-1}	block 7 density in $barn^{-1}$ cm^{-1}	block 8 density in $barn^{-1}$ cm^{-1}	block 9 density in $barn^{-1}$ cm^{-1}
92234	9,56E-07	1,01E-06	9,68E-07	1,05E-06	4,85E-07	1,14E-06	5,70E-07	1,08E-06	1,06E-06
92235	7,99E-05	9,79E-05	8,37E-05	0,000114	3,77E-05	0,000155	7,17E-05	0,000127	0,000117
92236	1,38E-05	1,11E-05	1,32E-05	8,71E-06	7,51E-06	2,19E-06	2,39E-06	6,72E-06	8,17E-06
92237	4,99E-09	4,35E-09	4,61E-09	3,46E-09	3,43E-09	1,08E-09	1,10E-09	2,00E-09	3,60E-09
92238	0,00064	0,000642	0,00064	0,000644	0,000329	0,000647	0,000332	0,000645	0,000644
93237	3,23E-07	2,03E-07	2,92E-07	1,13E-07	1,68E-07	4,25E-09	1,35E-08	6,82E-08	1,02E-07
93239	2,35E-08	2,42E-08	2,23E-08	2,41E-08	1,57E-08	2,90E-08	1,38E-08	1,77E-08	2,61E-08
94238	3,72E-08	1,71E-08	3,16E-08	6,88E-09	2,06E-08	3,30E-11	3,53E-10	2,96E-09	5,70E-09
94239	3,77E-06	3,36E-06	3,67E-06	2,67E-06	1,79E-06	4,48E-07	6,71E-07	2,19E-06	2,59E-06
94240	8,13E-07	5,37E-07	7,51E-07	3,26E-07	4,14E-07	7,01E-09	3,54E-08	1,91E-07	2,87E-07
94241	2,91E-07	1,65E-07	2,61E-07	7,43E-08	1,46E-07	2,29E-10	3,66E-09	3,33E-08	6,25E-08
94242	4,92E-08	1,78E-08	4,04E-08	5,40E-09	3,02E-08	1,65E-12	1,05E-10	1,63E-09	4,00E-09
95241	1,43E-08	5,07E-09	1,05E-08	1,74E-09	4,77E-09	4,28E-13	2,50E-11	4,99E-10	1,96E-09
95242	0	0	0	0	0	0	0	0	0
95243	2,06E-09	5,52E-10	1,58E-09	1,12E-10	1,27E-09	4,05E-15	8,45E-13	2,39E-11	7,85E-11
96242	5,04E-09	1,06E-09	3,10E-09	2,39E-10	1,77E-09	5,92E-15	1,30E-12	4,07E-11	3,38E-10
96243	3,39E-11	4,99E-12	1,97E-11	7,37E-13	1,33E-11	2,23E-18	1,73E-15	8,98E-14	1,12E-12
96244	1,51E-10	2,87E-11	1,07E-10	3,85E-12	9,64E-11	1,64E-17	1,15E-14	5,96E-13	2,54E-12
96245	1,89E-12	2,95E-13	1,28E-12	2,83E-14	1,11E-12	3,95E-20	3,67E-17	3,38E-15	1,82E-14
53135	1,33E-09	1,43E-09	1,25E-09	1,72E-09	8,95E-10	2,39E-09	1,22E-09	1,40E-09	1,71E-09
54135	6,81E-10	7,91E-10	6,84E-10	9,12E-10	3,58E-10	1,23E-09	5,89E-10	8,88E-10	9,37E-10
58141	1,41E-07	1,53E-07	1,34E-07	1,71E-07	9,35E-08	1,86E-07	1,27E-07	1,65E-07	1,76E-07
58142	4,19E-06	3,24E-06	3,99E-06	2,42E-06	2,33E-06	3,24E-07	5,74E-07	1,76E-06	2,24E-06
58144	9,53E-07	1,12E-06	1,09E-06	1,08E-06	7,18E-07	2,84E-07	4,20E-07	1,02E-06	7,68E-07
59143	6,02E-08	6,52E-08	5,64E-08	7,77E-08	3,98E-08	1,05E-07	5,52E-08	6,50E-08	7,78E-08
60143	3,53E-06	2,83E-06	3,42E-06	2,18E-06	1,83E-06	2,24E-07	5,10E-07	1,63E-06	2,03E-06
60144	1,45E-05	2,32E-06	1,41E-05	1,40E-06	1,95E-06	2,32E-08	1,38E-07	7,41E-07	1,51E-06
60145	2,80E-06	2,13E-06	2,67E-06	1,61E-06	1,50E-06	2,19E-07	3,85E-07	1,18E-06	1,49E-06
60146	2,27E-06	1,73E-06	2,15E-06	1,28E-06	1,27E-06	1,67E-07	2,98E-07	9,22E-07	1,18E-06
60147	4,32E-05	2,03E-08	4,32E-05	2,42E-08	1,25E-08	3,31E-08	1,70E-08	2,00E-08	2,42E-08
60148	1,23E-06	9,47E-07	1,17E-06	7,08E-07	6,83E-07	9,45E-08	1,68E-07	5,15E-07	6,55E-07
61147	0,052106	7,58E-07	0,052106	6,48E-07	4,82E-07	9,01E-08	1,83E-07	5,30E-07	5,24E-07
61148	1,56E-07	2,31E-09	1,56E-07	1,99E-09	2,01E-09	2,75E-10	6,29E-10	1,21E-09	1,68E-09
61148	2,16E-05	7,82E-15	2,16E-05	7,08E-15	4,50E-15	3,96E-15	2,92E-15	5,88E-15	6,97E-15
61149	1,54E-07	1,60E-09	1,54E-07	1,89E-09	1,03E-09	2,54E-09	1,31E-09	1,52E-09	1,88E-09

62147	5,59E-07	3,08E-07	4,56E-07	1,76E-07	2,33E-07	1,57E-09	1,34E-08	8,39E-08	2,48E-07
62148	8,67E-05	1,63E-07	8,66E-05	8,61E-08	1,64E-07	7,69E-10	7,91E-09	4,57E-08	6,96E-08
62149	6,80E-09	8,15E-09	7,14E-09	8,92E-09	3,27E-09	1,11E-08	5,48E-09	9,81E-09	9,31E-09

Table 6 Specifics for core block 10 until 18

Isotope number	block 10 density in barn^{-1} cm^{-1}	block 11 density in barn^{-1} cm^{-1}	block 12 density in barn^{-1} cm^{-1}	block 13 density in barn^{-1} cm^{-1}	block 14 density in barn^{-1} cm^{-1}	block 15 density in barn^{-1} cm^{-1}	block 16 density in barn^{-1} cm^{-1}	block 17 density in barn^{-1} cm^{-1}	block 18 density in barn^{-1} cm^{-1}
92234	1,08E-06	1,10E-06	1,06E-06	1,03E-06	5,10E-07	1,13E-06	5,42E-07	1,07E-06	9,64E-07
92235	0,000128	0,000135	0,000119	0,000108	4,60E-05	0,000148	5,86E-05	0,000123	8,22E-05
92236	6,56E-06	5,42E-06	7,91E-06	9,64E-06	6,29E-06	3,31E-06	4,41E-06	7,25E-06	1,35E-05
92237	3,45E-09	2,59E-09	2,41E-09	3,88E-09	2,94E-09	1,65E-09	1,92E-09	2,10E-09	4,93E-09
92238	0,000645	0,000646	0,000644	0,000643	0,00033	0,000647	0,000331	0,000644	0,00064
93237	6,38E-08	4,24E-08	9,65E-08	1,44E-07	1,13E-07	1,34E-08	5,22E-08	8,07E-08	2,99E-07
93239	3,07E-08	2,75E-08	1,81E-08	2,47E-08	1,55E-08	2,88E-08	1,37E-08	1,73E-08	2,36E-08
94238	2,72E-09	1,41E-09	5,20E-09	1,00E-08	1,07E-08	2,24E-10	3,04E-09	3,89E-09	3,29E-08
94239	2,13E-06	1,75E-06	2,55E-06	2,95E-06	1,63E-06	9,35E-07	1,26E-06	2,37E-06	3,67E-06
94240	1,81E-07	1,16E-07	2,74E-07	4,05E-07	2,99E-07	3,11E-08	1,46E-07	2,28E-07	7,64E-07
94241	3,17E-08	1,62E-08	5,78E-08	1,04E-07	9,10E-08	2,16E-09	3,13E-08	4,37E-08	2,67E-07
94242	1,48E-09	5,63E-10	3,60E-09	8,92E-09	1,29E-08	3,45E-11	2,35E-09	2,39E-09	4,24E-08
95241	3,48E-10	1,47E-10	1,24E-09	2,56E-09	2,27E-09	8,84E-12	5,11E-10	7,89E-10	1,10E-08
95242	0	0	0	0	0	0	0	0	0
95243	2,19E-11	6,43E-12	6,71E-11	2,17E-10	4,09E-10	1,84E-13	4,43E-11	3,91E-11	1,68E-09
96242	3,16E-11	9,56E-12	1,33E-10	4,12E-10	5,84E-10	2,72E-13	6,80E-11	7,53E-11	3,46E-09
96243	7,22E-14	1,63E-14	3,67E-13	1,49E-12	3,23E-12	2,22E-16	2,17E-13	1,82E-13	2,29E-11
96244	5,32E-13	1,20E-13	2,08E-12	8,83E-12	2,29E-11	1,60E-15	1,44E-12	1,09E-12	1,15E-10
96245	2,98E-15	5,32E-16	1,43E-14	7,45E-14	2,24E-13	3,62E-18	9,69E-15	6,73E-15	1,38E-12
53135	2,21E-09	2,01E-09	1,25E-09	1,68E-09	1,03E-09	2,33E-09	1,07E-09	1,36E-09	1,34E-09
54135	1,07E-09	1,07E-09	8,25E-10	8,78E-10	4,24E-10	1,19E-09	4,99E-10	8,65E-10	6,93E-10
58141	2,35E-07	2,20E-07	1,38E-07	1,74E-07	1,08E-07	2,34E-07	1,12E-07	1,55E-07	1,40E-07
58142	1,71E-06	1,34E-06	2,15E-06	2,73E-06	1,89E-06	6,73E-07	1,24E-06	1,94E-06	4,07E-06
58144	1,08E-06	9,13E-07	1,03E-06	1,15E-06	7,45E-07	5,44E-07	6,57E-07	1,02E-06	1,07E-06
59143	1,01E-07	9,22E-08	5,70E-08	7,64E-08	4,63E-08	1,07E-07	4,80E-08	6,30E-08	6,03E-08
60143	1,55E-06	1,22E-06	1,98E-06	2,43E-06	1,58E-06	5,69E-07	1,10E-06	1,78E-06	3,46E-06
60144	6,23E-07	4,02E-07	1,15E-06	1,68E-06	1,31E-06	1,01E-07	6,13E-07	9,24E-07	1,42E-05
60145	1,14E-06	8,97E-07	1,43E-06	1,81E-06	1,23E-06	4,53E-07	8,20E-07	1,29E-06	2,72E-06
60146	8,95E-07	6,98E-07	1,13E-06	1,45E-06	1,01E-06	3,48E-07	6,51E-07	1,01E-06	2,19E-06
60147	3,12E-08	2,84E-08	1,77E-08	2,37E-08	1,44E-08	3,29E-08	1,49E-08	1,94E-08	4,32E-05
60148	5,00E-07	3,92E-07	6,29E-07	7,99E-07	5,53E-07	1,96E-07	3,62E-07	5,65E-07	1,19E-06
61147	5,20E-07	4,22E-07	6,03E-07	7,07E-07	0,208422	2,13E-07	3,50E-07	5,63E-07	0,052106
61148	1,95E-09	1,41E-09	1,38E-09	2,23E-09	3,10E-07	7,21E-10	1,24E-09	1,27E-09	1,56E-07
61148	6,94E-15	6,07E-15	6,00E-15	7,57E-15	4,32E-05	5,02E-15	3,73E-15	6,05E-15	2,16E-05
61149	2,41E-09	2,18E-09	1,36E-09	1,86E-09	3,06E-07	2,49E-09	1,17E-09	1,48E-09	1,54E-07
62147	6,61E-08	4,15E-08	1,41E-07	2,10E-07	1,52E-07	8,84E-09	6,81E-08	1,10E-07	4,86E-07
62148	4,19E-08	2,50E-08	6,96E-08	1,13E-07	0,000173	5,07E-09	4,25E-08	5,59E-08	8,66E-05
62149	9,82E-09	1,03E-08	9,51E-09	8,59E-09	3,83E-09	1,09E-08	4,67E-09	9,60E-09	6,97E-09

Table 7 Specifics for core block 19 and 20

Isotope number	block 19 density in barn^{-1} cm^{-1}	block 20 density in barn^{-1} cm^{-1}
92234	9,87E-07	9,88E-07
92235	9,04E-05	9,06E-05
92236	1,23E-05	1,22E-05
f92237	4,67E-09	4,18E-09
92238	0,000641	0,000641
93237	2,45E-07	2,45E-07
93239	2,39E-08	2,15E-08
94238	2,35E-08	2,35E-08
94239	3,51E-06	3,51E-06
94240	6,45E-07	6,43E-07
94241	2,12E-07	2,11E-07
94242	2,76E-08	2,78E-08
95241	7,41E-09	7,27E-09
95242	0	0
95243	9,63E-10	9,72E-10
96242	1,90E-09	1,77E-09
96243	1,07E-11	9,65E-12
96244	5,68E-11	5,80E-11
96245	6,29E-13	6,44E-13
53135	1,34E-09	1,27E-09
54135	7,37E-10	7,19E-10
58141	1,47E-07	1,42E-07
58142	3,64E-06	3,63E-06
58144	1,12E-06	1,15E-06
59143	6,10E-08	5,81E-08
60143	3,19E-06	3,18E-06
60144	1,36E-05	1,36E-05
60145	2,45E-06	2,45E-06
60146	1,95E-06	1,94E-06
60147	4,32E-05	4,32E-05
60148	1,06E-06	1,06E-06
61147	0,052106	0,052106
61148	1,56E-07	1,56E-07
61148	2,16E-05	2,16E-05
61149	1,54E-07	1,54E-07
62147	3,84E-07	3,65E-07
62148	8,66E-05	8,66E-05
62149	7,66E-09	7,60E-09